Journal of Instrumentation

SISSA

PAPER • OPEN ACCESS

Muon identification using multivariate techniques in the CMS experiment in proton-proton collisions at sqrt(*s*) = 13 TeV

To cite this article: A. Hayrapetyan *et al* 2024 *JINST* **19** P02031

View the article online for updates and enhancements.

You may also like

- Searching for solar KDAR with DUNE
The DUNE collaboration, A. Abed Abud, B. Abi et al.
- Identification of hadronic tau lepton decays using a deep neural network
A. Tumasyan, W. Adam, J.W. Andrejkovic et al.

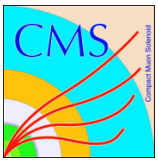


This content was downloaded from IP address 193.140.54.155 on 13/03/2024 at 18:16

Published by IOP Publishing for Sissa Medialab

Received: *October 5, 2023*
Accepted: *November 2, 2023*
Published: *February 23, 2024*

Muon identification using multivariate techniques in the CMS experiment in proton-proton collisions at $\sqrt{s} = 13$ TeV



The CMS collaboration

E-mail: cms-publication-committee-chair@cern.ch

Abstract: The identification of prompt and isolated muons, as well as muons from heavy-flavour hadron decays, is an important task. We developed two multivariate techniques to provide highly efficient identification for muons with transverse momentum greater than 10 GeV. One provides a continuous variable as an alternative to a cut-based identification selection and offers a better discrimination power against misidentified muons. The other one selects prompt and isolated muons by using isolation requirements to reduce the contamination from nonprompt muons arising in heavy-flavour hadron decays. Both algorithms are developed using 59.7 fb^{-1} of proton-proton collisions data at a centre-of-mass energy of $\sqrt{s} = 13$ TeV collected in 2018 with the CMS experiment at the CERN LHC.

Keywords: Muon spectrometers; Particle identification methods; Particle tracking detectors

ArXiv ePrint: 2310.03844

© 2024 CERN for the benefit of the CMS collaboration. Published by IOP Publishing Ltd on behalf of Sissa Medialab. Original content from this work may be used under the terms of the Creative Commons Attribution 4.0 licence. Any further distribution of this work must maintain attribution to the author(s) and the title of the work, journal citation and DOI.

https://doi.org/10.1088/1748-0221/19/02/P02031

2024 JINST 19 P02031

Contents

1 Introduction **1**

2 The CMS detector **2**

3 Data and simulated samples **3**

4 Muon reconstruction, identification, and isolation **4**

5 Definition of the multivariate discriminators **6**
5.1 General muon identification 6
5.2 Prompt-muon identification and isolation 9

6 Performance in data **10**
6.1 Muon MVA ID performance 13
6.2 Prompt-muon MVA performance 13

7 Summary **17**

The CMS collaboration **22**

2024 JINST 19 P02031

1 Introduction

Accurate measurements of processes with muons in the final state are among the main goals of the CMS experiment [1] at the CERN LHC. Because many analyses rely on the presence of these leptons to identify interesting physical processes and suppress backgrounds, a successful physics program relies on a high-quality muon selection. First, it is necessary to discriminate genuine muons from other background sources that fake muons, such as spurious hits misreconstructed as muons, or misidentified charged hadrons. Then, for analyses targeting prompt muons from decays of the W, Z, or Higgs bosons, or muons from τ lepton decays, it is important to avoid a contamination from nonprompt muons produced by hadron decays, especially b quark hadrons.

The LHC Run 2 at CERN occurred during the years 2015 to 2018 and provided an unprecedented number of proton-proton (pp) collision events at a centre-of-mass energy, $\sqrt{s}$, of 13 TeV recorded by the CMS experiment. During this period, muon identification relied on a cut-based approach, using a set of requirements on individual variables related to the information from the tracker and the muon system. This approach defines three sets of selection criteria [2] with a differing balances between efficiency and purity that allow each analysis to choose the desired set. However, whenever the purity of the selected sample is critical, or the muon identification performance is degraded due to the number of simultaneous collisions in the same or adjacent bunch crossings (pileup, PU),

the use of more sophisticated techniques is crucial to maintain an acceptable compromise between efficiency and purity.

We adopted a multivariate analysis (MVA) approach to design two muon identification discriminators. The first discriminator, referred to as "muon MVA ID", is used for generic muon identification while minimizing hadron misidentification. This discriminator has been trained using muon identification variables defined in ref. [2] and is presented in this paper for the first time. The second MVA, referred to as the "prompt-muon MVA", is designed to accurately identify isolated prompt muons, for those particular cases in which it is critical to tag such muons, particularly those produced from the decays of W, Z, Higgs bosons, or τ leptons.

The prompt-muon MVA discriminator was trained in the context of multileptonic analyses with high yields of nonprompt backgrounds, and it was already used in several CMS analyses with multilepton final states [3–10]. This prompt-muon MVA was designed for isolated muons and it was trained using both muon identification and isolation variables. Hence, it cannot be used to identify other genuine muons, such as muons from heavy-flavour decays.

Following a similar MVA approach, a second classifier was trained, combining only muon identification variables, to construct a more general and robust discriminator able to outperform the cut-based identification [2]. Such a discriminator could offer a continuous variable that provides more flexibility to pick the desired trade-off between signal and background efficiencies. With these goals in mind, we developed the muon MVA ID discriminator for muons with transverse momentum (p_T) >10 GeV and plan to use it for the Run 3 era of the LHC running. Low-p_T muons come from low-mass resonances, so they present different signatures when compared to muons from Z bosons, hence they require special treatment and are beyond the scope of this study. For identification of low-p_T muons, a special MVA-based discriminator, referred to as "Soft MVA ID" [11], was developed and used during Run 2. It was trained using the 2016 data set for muons with $p_T < 10$ GeV. We present technical aspects about the training of the two algorithms in this paper and compare their performance in data and simulated events.

The paper is organized as follows: section 2 briefly describes the CMS experiment, and section 3 summarizes the data and simulated samples used in this work. Section 4 contains the details of the event reconstruction. Section 5 provides a full description of the MVA discriminators, together with the details of their training. Section 6 discusses the performance of the algorithms on the Run 2 data and Monte Carlo (MC) simulation. The results are summarized in section 7.

2 The CMS detector

The central feature of the CMS apparatus is a superconducting solenoid of 6 m internal diameter, providing a magnetic field of 3.8 T. Within the solenoid volume there are a silicon pixel and strip tracker, a lead tungstate crystal electromagnetic calorimeter, and a brass and scintillator hadron calorimeter, each composed of a barrel and two endcap sections. Forward calorimeters extend the pseudorapidity (η) coverage provided by the barrel and endcap detectors. Muons are measured in gas-ionization detectors embedded in the steel flux-return yoke outside the solenoid. A more detailed description of the CMS detector, together with a definition of the coordinate system used and the relevant kinematic variables, is reported in ref. [1].

2024 JINST 19 P02031

The CMS muon system consists of three types of gas-ionization detectors: drift tube chambers (DTs), cathode strip chambers (CSCs), and resistive-plate chambers (RPCs). The DT and CSC detectors are located in the regions of $|\eta| < 1.2$ and $0.9 < |\eta| < 2.4$, respectively, and are complemented by the RPCs in the range $|\eta| < 1.9$. The chambers are arranged to maximize the coverage and to provide some overlap wherever possible. In both the barrel and endcap regions, the chambers are grouped into four "muon stations", separated by the steel absorber of the flux-return yoke. A detailed description of these detectors, including the gas composition and operating voltage, is reported in ref. [2]. Figure 1 shows a schematic representation of the CMS detector.

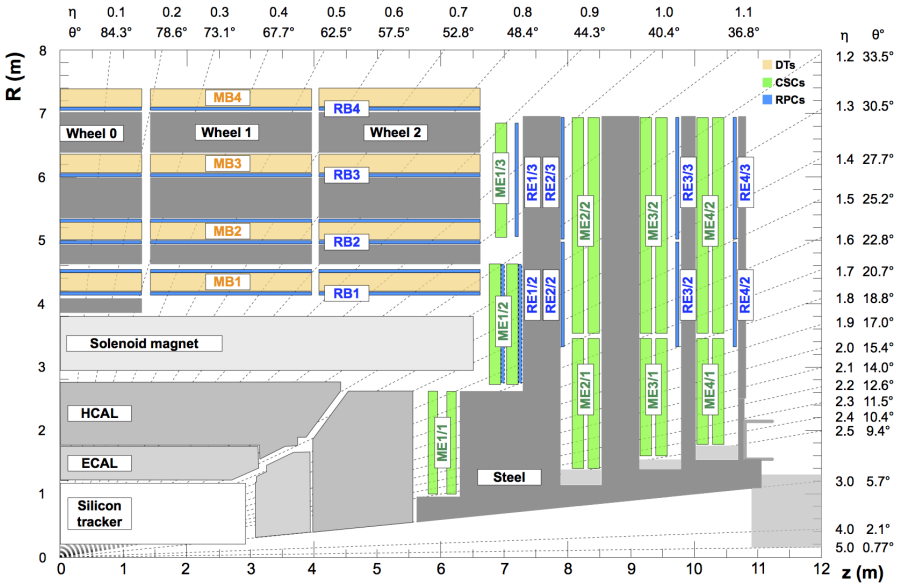


Figure 1. Layout of a quadrant of the CMS detector with the muon system highlighted. The chambers are named MB for muon barrel, corresponding to DT chambers, and ME for muon endcap, corresponding to CSC chambers. The RPC chambers are named RB and RE for barrel and endcaps, respectively. Reproduced from [2]. © 2018 CERN for the benefit of the CMS collaboration. CC BY 3.0.

Events of interest are selected using a two-tiered trigger system. The first level, composed of custom hardware processors, uses information from the calorimeters and muon detectors to select events at a rate of around 100 kHz within a fixed latency of about 4 μs [12]. The second level, known as the high-level trigger, consists of a farm of processors running a version of the full event reconstruction software optimized for fast processing, and reduces the event rate to around 1 kHz before data storage [13].

3 Data and simulated samples

The studies described in this paper are based on a data set of pp collisions at $\sqrt{s} = 13$ TeV produced at the LHC in 2018 and corresponding to an integrated luminosity of 59.7 fb^{-1} [14, 15] recorded using the CMS experiment. The 2018 data set is representative of the Run 2 data-taking conditions. The trigger required the presence of a muon with a $p_{\mathrm{T}} > 24$ GeV threshold fulfilling loose isolation requirements [16].

2024 JINST 19 P02031

Events are simulated representing the main standard model (SM) processes and matching the detector and PU conditions of the 2018 data-taking period. Drell-Yan (DY) dilepton events are generated at next-to-leading order (NLO) in perturbative quantum chromodynamics (QCD) using the MadGraph5_aMC@NLO 2.6.1 generator [17, 18]. The POWHEG 2.0 [19–21] generator at NLO accuracy in QCD is used to simulate top quark pair production ($t\bar{t}$) and the production of a Higgs boson in association with a top quark pair ($t\bar{t}H$). Samples of Z + jets, W + jets, and multijet events are generated at leading order (LO) in QCD using the MadGraph5_aMC@NLO generator. For all the MC simulated samples, the primary interaction is overlaid with additional simulated minimum-bias events to simulate the effect of the PU. The NNPDF 3.1 next-to-NLO [22] parton distribution function set is used for generating all MC samples. Parton showering and hadronization are simulated with PYTHIA v8.240 [23, 24] using the underlying event tune CP5 [25]. In the event simulation using MadGraph5_aMC@NLO, the FxFx [26] (MLM [18]) merging scheme is used for NLO (LO) samples, to avoid possible double-counting of jets from the matrix element calculations and parton shower. The generated events are then processed through a detailed simulation of the CMS detector based on Geant4 10.04 [27] and are reconstructed with the same algorithms as used for data.

For the training and misidentification rate studies for the muon MVA ID, two different $t\bar{t}$ samples that include semileptonic decays are used. The simulated sample used to check the performance includes generation-level information for the particles produced in the PU interactions, whereas the other sample does not. The choice of a $t\bar{t}$ sample for the training provides a wide variety of sources of genuine muons, including muons from prompt decays and from heavy-flavour hadron decays. To determine the source of muons in simulated events we look for the geometrical matching between the hits of the simulated muon track and those of the muon track reconstructed in the muon system. From the simulated muon track we are able to trace the generated parent particle. In the simulated $t\bar{t}$ sample used to check the performance, we find that 60% of muons with $p_T > 10\,\text{GeV}$ passing the loose cut-based identification criteria [2] are prompt isolated muons originating from the primary interaction (gauge boson decays); 8% are isolated muons from τ lepton decays; 30% are nonisolated muons from heavy-flavour decays (b and c hadrons); and 2% are muons from light-hadron decays (pions or kaons) or nonprompt muon candidates from hadron misreconstruction.

4 Muon reconstruction, identification, and isolation

In the standard CMS reconstruction procedure for pp collisions, muon tracks are first reconstructed independently in the inner tracker and in the muon systems. In the muon system, tracks called "standalone muons" are reconstructed by using information from the DT, CSC, and RPC detectors along the muon trajectory using the Kalman filtering technique [28]. Within each station, multiple detector planes record muon hits. The hits within a station are combined into segments, which are in turn fitted into standalone-muon tracks. If the momentum, direction, and position in the transverse plane of a standalone-muon tracks and a track reconstructed in the inner tracker [29] are compatible, then a global track is fitted by combining hits from the tracker track and standalone-muon track in a common fit using the Kalman filtering method, referred to as "global muons". A third type of muons referred to as "tracker muons" are reconstructed by extrapolating the inner tracker tracks outward to the muon system with loose geometrical matching to the DT or CSC segments, these muons need to have a p_T of at least 3 GeV, otherwise they would not be able to reach the first station in the muon

2024 JINST 19 P02031

system. If at least one muon segment matches the extrapolated track, the track is qualified as a "tracker muon". Tracker muons have higher efficiency than global muons for low muon momenta and in regions of the CMS detector that are less instrumented. More details about muon reconstruction and the corresponding track parameter resolution of each muon type are reported in refs. [2, 30].

The primary vertex (PV) is taken to be the vertex corresponding to the hardest scattering in the event, evaluated using tracking information alone, as described in section 9.4.1 of ref. [31]. The performance of the PV determination depends on the p_{T} of the particles, as described in ref. [29].

Reconstructed muons are an input into the CMS particle-flow (PF) algorithm [32], which reconstructs and identifies each individual particle in an event by combining the information from all the CMS subdetectors. Particles reconstructed by the PF algorithm are classified into charged and neutral hadrons, photons, electrons, and muons.

After reconstruction, hadrons are clustered into jets using the anti-k_{T} algorithm [33, 34] with a distance parameter of 0.4. For this analysis, only jets with $p_{\mathrm{T}} > 10\,\mathrm{GeV}$ are selected. Charged hadrons not associated with the PV are excluded from the clustering. The energy of the reconstructed jets is corrected for residual PU effects using the method described in refs. [35, 36] and calibrated as a function of jet p_{T} and η [37]. Jets originating from the hadronization of b quarks are identified with the DeepJet b tagging algorithm [38, 39]. We define the nearest jet to the muon as the one in which the muon candidate is clustered.

In the following we describe the standard CMS muon identification method, which makes use of a set of variables related to the muon track candidate information from both the tracker and the muon system. The most common sets of selection criteria are referred to as loose, medium, and tight. Their efficiencies, as measured during the Run 2 data taking by selecting muons with $p_{\mathrm{T}} > 20\,\mathrm{GeV}$, are 99.75, 98.25, and 96.00% with statistical uncertainties between 0.02 and 0.03% for muons with $|\eta| < 0.9$. Then, for muons with $|\eta| > 0.9$ the efficiencies for each WP are 99.77, 98.55, and 97.46% with the statistical uncertainties between 0.02 and 0.04%[2].

The "relative isolation" variable is used to distinguish between muons from heavy-flavour decays and the prompt muons. It is defined as the p_{T} sum of all charged hadrons, the transverse energies of all photons and of all neutral hadrons reconstructed by the PF algorithm in a cone of angle $\Delta R = \sqrt{(\Delta\phi)^2 + (\Delta\eta)^2}$ around the muon direction, divided by the muon p_{T}, where ϕ is the azimuthal angle. The charged PF particles not associated with the PV are not included in this sum, whereas the contribution from neutral particles arising from PU is taken into account by using the following two alternative approaches [2]. In the first approach, the corrected energy sum from neutral particles is obtained by subtracting the sum of charged-hadron deposits originating from PU vertices scaled by a factor of 0.5 from the energy sum of neutral hadrons and photons [2]. In the second approach, the sums are corrected using the average energy density in the event (ρ) [40], scaled by the corresponding "effective area" ($\mathcal{A}$). If the correction exceeds the PF cluster sum, the correction to the isolation is set to zero. Effective areas are determined independently for the electromagnetic and the hadronic energy sums and separately in barrel and endcap components.

For this study, two isolation variables are used: one computed with all the PF particles within an $\Delta R = 0.4$ cone and corrected using the first method, and the other, referred to as "mini-isolation" [41], for which the cone size varies as a function of the muon p_{T}: $\Delta R = 0.2$ when $p_{\mathrm{T}} < 50\,\mathrm{GeV}$, $\Delta R = 10\,\mathrm{GeV}/p_{\mathrm{T}}$ when $50 < p_{\mathrm{T}} < 200\,\mathrm{GeV}$, and $\Delta R = 0.05$ otherwise, corrected

2024 JINST 19 P02031

using the second method. This variable is particularly well suited to identify isolated muons in events with significant hadronic activity or in the Lorentz-boosted regime where accidental overlaps of muons and jets may occur, but still performs just as well in cleaner environments.

5 Definition of the multivariate discriminators

Two classifiers using MVA techniques are presented. Muons used in the training of both classifiers must pass the loose cut-based identification criteria and have $p_{\mathrm{T}} > 10$ (5) GeV for the muon MVA ID (prompt-muon MVA). The loose identification criteria requires muons selected by the PF algorithm to be either global muons or tracker muons. This preselection shows an efficiency of almost 100% and helps to avoid poorly reconstructed muons that are not relevant for analyses.

5.1 General muon identification

The muon MVA ID discriminant is trained to distinguish genuine (i.e. signal) muons from background muons. Signal muons are produced promptly in the decay of W, Z, and Higgs bosons, isolated muons from τ leptons decays, and nonisolated muons from heavy-flavour hadron decays. Background muons come from light hadron (i.e. kaons and pions) decays and spurious signatures in the detector misreconstructed as muons, such as hadrons detected in the muon system after traversing the calorimeters and the steel flux-return yoke.

The sources of the muons included in the training sample are shown as a function of p_{T} and η in figure 2. As expected, the various signal contributions, as well as the background, exhibit different p_{T} profiles. The low-p_{T} region is enriched in muons from heavy-flavour hadron decays and background sources, whereas the higher p_{T} region presents a larger proportion of muons originating from prompt decays.

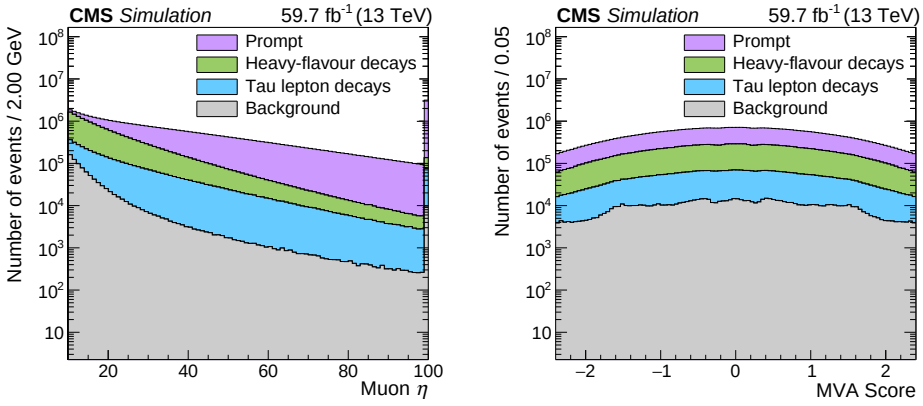


Figure 2. Composition of the simulated $\mathrm{t\bar{t}}$ sample used for training after muon preselection in terms of muon origin according to generator-level information. The composition is shown as a function of p_{T} (left) and η (right). The last bin on the left figure includes events with $p_{\mathrm{T}} > 100$ GeV.

The training of the MVA is performed with all variables used in the standard cut-based identification criteria, with the exception of the compatibility with the PV, quantified with the muon impact parameter in the xy-plane and along the z-direction. These variables are excluded as we aim

2024 JINST 19 P02031

to obtain a discriminator to select both prompt and nonprompt muons produced in heavy-flavour hadron decays. To discard nonprompt muons, further isolation requirements or a custom impact parameter selection criteria should be applied at the analysis level. The input variables used are:

- The p_{T} and η of the muon.
- "Global muon" flag.
- Normalized χ^2 of the muon track fit.
- Number of muon stations with hits included in the muon track fit.
- χ^2 of the kink-finder algorithm on the inner track defined in ref. [2]. The algorithm splits the inner track in two parts in several places along the trajectory and compares them. A large χ^2 indicates that the two parts are not compatible with being a single track.
- χ^2 of the position matching between the inner and standalone tracks (local χ^2). If there is no standalone track, it is set to 0.
- Segment compatibility: the compatibility of track segments in the muon system with the pattern expected for a minimum ionizing particle.
- Number of hits in the pixel detector used to fit the muon track.
- Number of tracker layers used in the muon track fit.
- Fraction of tracker hits used for the fit of the inner track.
- Number of matched stations: number of segments (one per station) reconstructed in the muon chambers and used in the global muon track fit.

The p_{T} and η bins are weighted to have the same distributions in both signal and background samples to avoid any kinematic bias in the muon classification. The distributions of the input variables used in the $\mathrm{t\bar{t}}$ training sample for signal and background muons passing the preselection requirements are shown in figure 3. For the three input variables defined as a χ^2 the logarithm of the variable is presented.

A random forest [42] classifier is trained using the Scikit-learn 0.19.1 package [43]. All the parameters of the model (hyperparameters) are optimized, combining manual and grid search strategies, with the aim of achieving the best performance while preventing overfitting, and hence reaching the highest possible accuracy on the classification. The optimal values of the hyperparameters are 200 trees with a maximum depth of 8. The optimization was performed using the area under the receiver operator characteristic (ROC) curve, as well as the efficiency and the background rejection. The memory usage was also taken into account in the optimization, so slightly higher performance was traded for lower memory consumption. The main challenge of this classification problem is the class imbalance, since the simulation contains many more signal than background muons. The most important input variables in the training are the χ^2 of the kink-finder algorithm on the inner track and the χ^2 of the position matching between the inner and standalone tracks.

The trained muon MVA ID discriminator offers a continuous variable, which provides flexibility to select the most suitable trade-off between signal and background efficiencies, known as working

2024 JINST 19 P02031

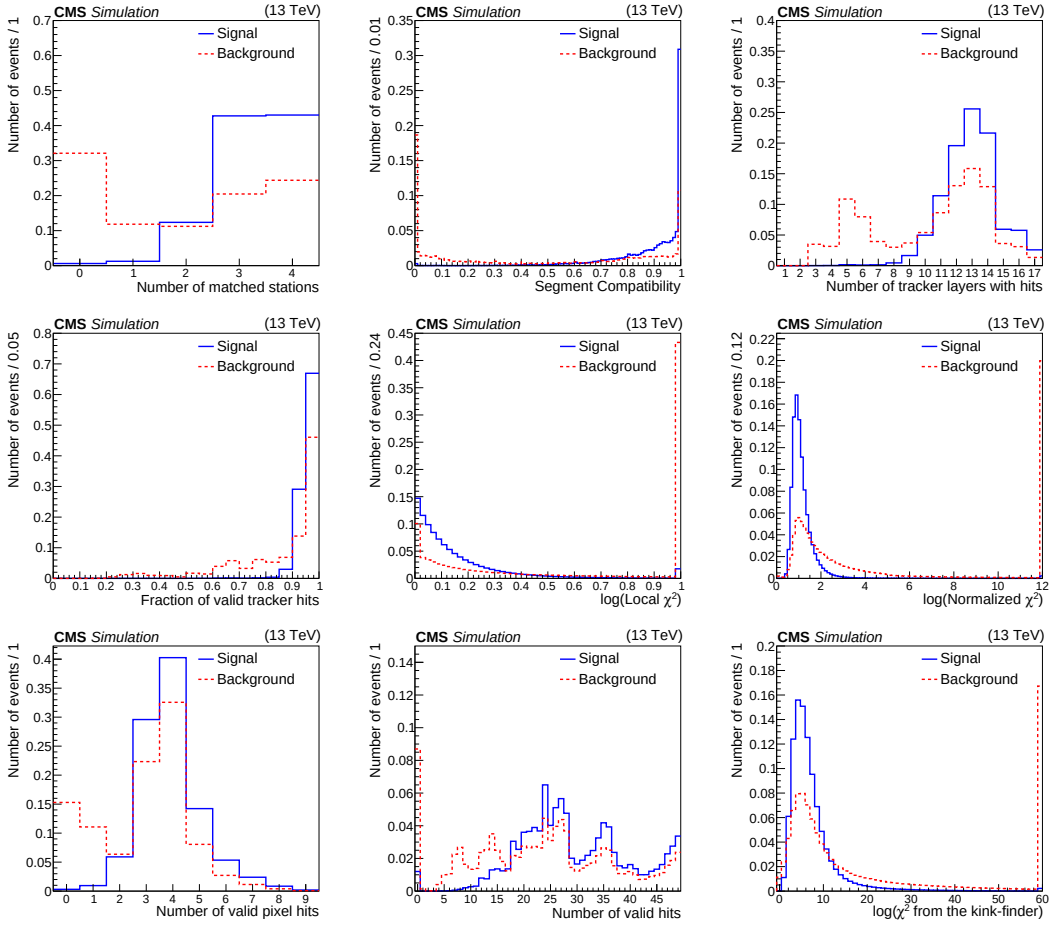


Figure 3. Distribution in the simulated $t\bar{t}$ training sample of the number of matched stations (upper left), the segment compatibility (upper central), the number of tracker layers with hits (upper right), the fraction of valid tracker hits (middle left), the inner-standalone matching (middle central) and normalized χ^2 of the muon fit (middle right), the number of valid pixel hits (lower left) and the total number of valid muon chamber hits (lower central), and the χ^2 of the kink-finder algorithm (lower right), shown for signal and background, as defined in section 5.1. The last bin of each distribution contains the overflow events.

point (WP), for each analysis. Additionally, two WPs, medium and tight, are defined to provide a simple way to see the performance of the MVA in data. They provide an alternative discriminator for high-efficiency WPs while not necessarily as relaxed as the medium cut-based identification. The medium WP is defined as the value yielding the same background rejection of the cut-based selection medium WP, calculated for muons with $p_T > 20$ GeV in the $t\bar{t}$ simulated sample used to check the performance. A higher threshold in the muon MVA ID discriminator defines the tight WP to further reduce the background contamination by 10% with respect to the medium WP, while still providing high efficiency. The defined thresholds correspond to MVA > 0.08 and 0.20 for the medium and tight WPs, respectively. Figure 4 shows the ROC curve of the muon MVA ID with the selected muon MVA ID WPs. The cut-based medium and tight WPs, as well as the soft MVA ID [11] ROC curve are also shown for reference. The rates shown are computed selecting muons with $p_T > 10$ GeV in the $t\bar{t}$ sample that is not used for training. This plot summarizes the performance for all the available muon IDs.

2024 JINST 19 P02031

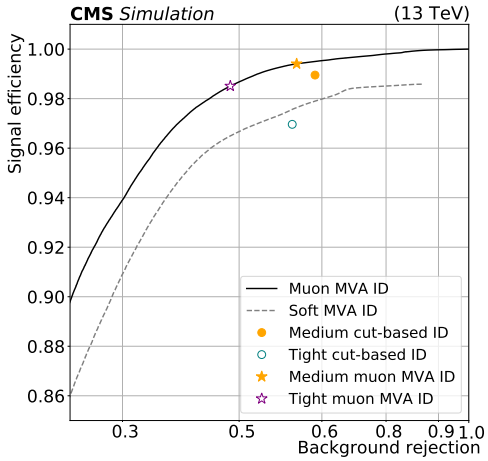


Figure 4. The ROC curve for muons with $p_T > 10$ GeV for the developed general muon MVA ID discriminator (black solid line) with the selected medium and tight WPs shown as orange solid and purple open stars, respectively. Orange solid and blue open points show the medium and tight WPs of the cut-based ID. The ROC curve of the soft MVA ID [11] is also shown (grey dashed line).

5.2 Prompt-muon identification and isolation

Muons originating from prompt decays of W, Z, or Higgs bosons, or from τ decays, appear isolated and pointing to the PV. This information is used to build an MVA discriminator that drastically reduces the contribution of nonprompt leptons to the selected muon sample. We refer to this discriminator as "prompt-muon MVA". In addition to the minimal selection criteria detailed at the beginning of the section, muons used in the training are required to have a mini-isolation smaller than 40% of the p_T of the muon. In addition, the muon impact parameter with respect to the PV is required to be smaller than 0.05 cm in the xy-plane and 0.1 cm in the z-direction. The three-dimensional impact parameter of the muon track with respect to the PV, divided by its uncertainty, which corresponds to its significance (d/σ_d) is required to be smaller than 8. These requirements reject muons that are very unlikely to have a prompt origin, while bounding some of the MVA input variables, enhancing its performance. The signal is defined as the muons selected by these criteria and matched to a generator-level muon produced in the prompt decay of the particles mentioned above, whereas all the muons not fulfilling these criteria are considered as background. The sample of signal (background) muons is obtained from simulated samples of $t\bar{t}H$ ($t\bar{t}$) events.

The input variables used in the training include properties of the muons, information regarding the muon isolation, and, if present, properties of the jet associated with the muon. To be considered as associated, the jet must contain the muon candidate. The training variables are:

- Muon p_T and $|\eta|$.
- Charged component of the mini-isolation variable, defined as $I_\mu^{\text{charged}} = \sum_{\text{charged}} p_T/p_T^\mu$.
- Neutral component of the mini-isolation variable, corrected for PU effects with the effective areas method [2], defined as $I_\mu^{\text{neutrals}} = \max\left(0, \sum_{\text{neutrals}} p_T - \rho\,\mathcal{A}\,(R/0.3)^2\right)/p_T^\mu$.

2024 JINST 19 P02031

- Muon-to-jet p_T ratio variable, p_T^{ratio}: the ratio of the transverse momentum of the muon to the transverse momentum of the nearest jet, p_T^{μ}/p_T^{jet}. If no jet associated to the muon is present, this variable is set to $1/(1 + I_{rel})$, where I_{rel} is the relative isolation.

- Muon relative p_T variable, p_T^{rel}: the component of the muon momentum in direction transverse to the jet, $p_T^{rel} = p^{\mu} \sin\theta$, where θ denotes the angle between the muon and jet momentum vectors and p^{μ}, the magnitude of the muon momentum. If no jet associated with the muon is present, this variable is set to zero.

- Jet b tagging score: the value of the DeepJet b tagging algorithm discriminator [38] of the associated jet. When such a jet is not present, the variable is set to zero.

- Jet charged constituents: the number, $N_{charged}$, of charged PF candidates within the associated jet. Tracks associated with those particles must be within $R < 0.4$ of the muon and are required to come from the PV to enter the counting. Minimal track quality, p_T, and impact parameter criteria are also applied. If such a jet does not exist this variable is set to zero.

- Longitudinal (d_z) and transverse (d_{xy}) impact parameters. Since these variables span over several orders of magnitude, their logarithmic value, $\log\left(d_{z(xy)}/1\,\text{cm}\right)$, is used.

- Significance of the three-dimensional impact parameter.

- Muon segment compatibility variable.

The classifier is trained using the TMVA 4.2.1 implementation [44] of a boosted decision tree (BDT) with gradient boosting. The distributions of signal and background muons, as predicted by the simulations, are shown in figure 5 as functions of the input variables. The hyperparameters of the BDT have been chosen to achieve the best performance: the algorithm used is a gradient boost with 1000 trees of maxium depth of 4. This optimization was performed using the area under the ROC curve as metric, since no WP was predefined.

The performance of the discriminator is shown in figure 6 together with the performance obtained using a cut-based approach, which combines a requirement on the tight or the medium cut-based identification WP with a range of requirements on the mini-isolation variable. For the prompt-muon MVA, a WP used already in ref. [3] is defined to have a MVA score larger than 0.85, which gives about 80% efficiency in the $t\bar{t}H$ events and a nonprompt muon rate of the order of 6×10^{-3} in $t\bar{t}$ events, where efficiency (nonprompt rate) is defined as the fraction of signal (background) muons passing the selection.

6 Performance in data

The performance of the discriminators is evaluated using both data and simulated events, and discussed in this section.

The efficiency is measured as a function of the muon p_T in two η regions using the "tag-and-probe method", which selects muons coming from the Z boson decay, as described in ref. [45]. Tag muons are required to pass the tight cut-based identification criteria and, to avoid any bias in the efficiency measurement, to be geometrically matched with the muon that triggered the event. Probe

2024 JINST 19 P02031

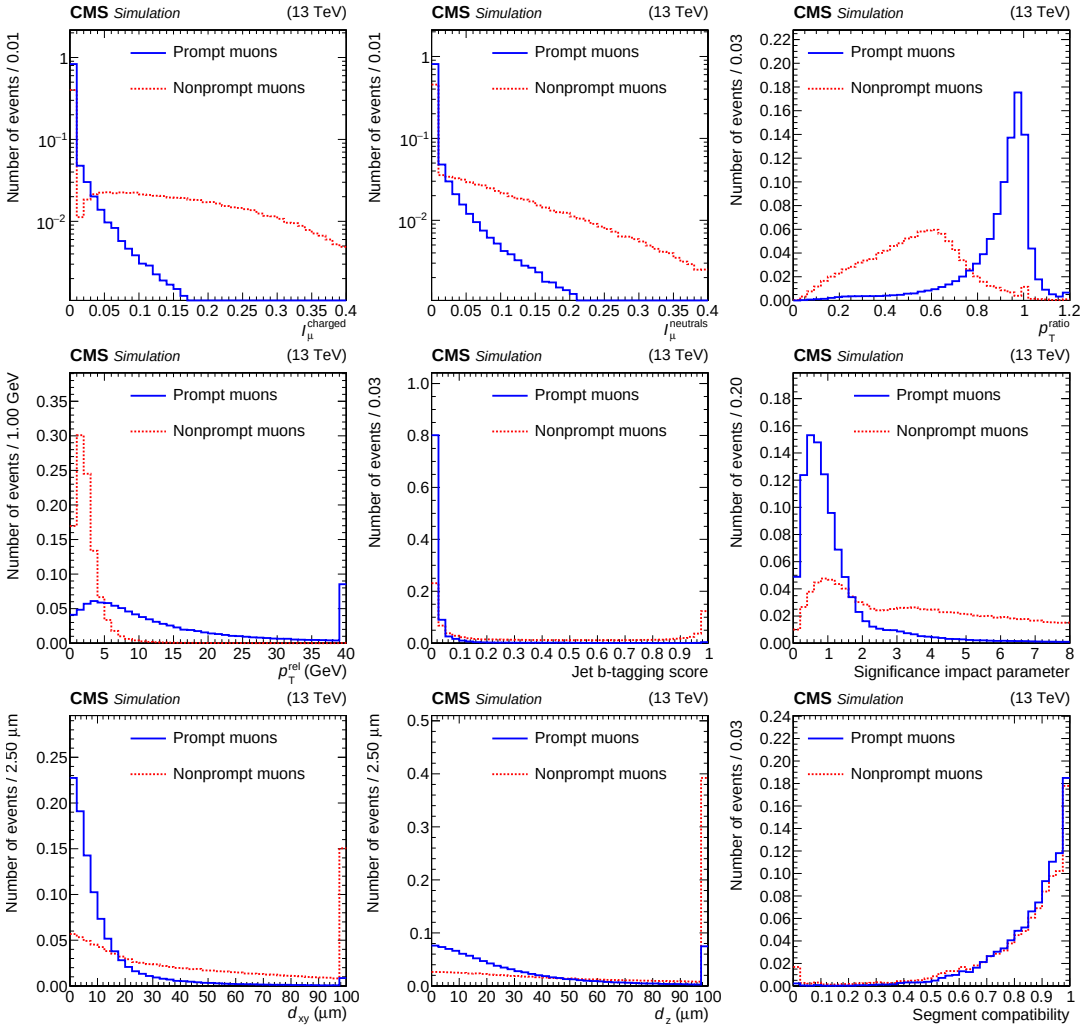


Figure 5. Simulated distributions of the charged component (upper left) and the neutral component (upper central) of mini-isolation, the muon to jet p_{T} ratio (upper right), the jet relative p_{T} (middle left), the score of the associated DeepJet b tagging algorithm (middle central), the significance of the impact parameter (middle right), the impact parameter in the transverse (lower left) and longitudinal (lower central) direction between the muon and the PV, and the segment compatibility (lower right) for prompt and nonprompt muons.

muons are required to pass the loose cut-based identification criteria. Efficiency is defined as the fraction of probe muons that pass the MVA identification requirement.

In simulation, any background to this selection is removed by requiring the tag and the probe muons to be produced by the decay of a Z boson, looking at the generation-level information. In collision events, a parametric model of the dimuon invariant mass distribution with a background and a signal component is built. The signal is parameterized using the templates predicted by the simulated sample of DY events convolved with a Gaussian distribution to account for potential resolution differences between data and simulation. To model the background, the convolution of an exponential decay distribution with an error function is used. The exponential is used to model the distribution at high-mass values whereas the error function is used to model the low-mass regime.

2024 JINST 19 P02031

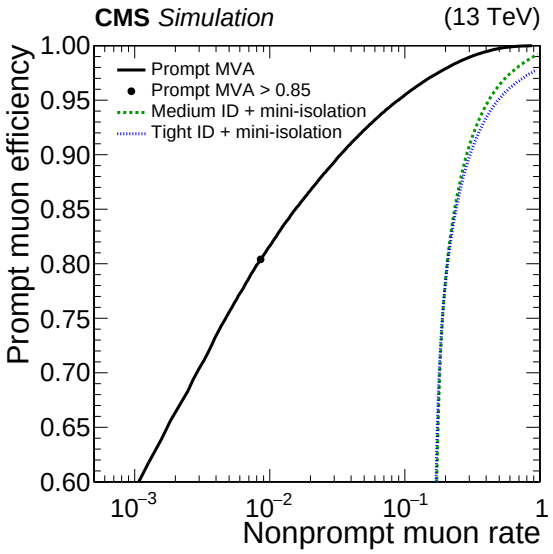


Figure 6. ROC curve for the prompt-muon MVA, and for the tight and medium cut-based criteria together with requirements on mini-isolation. For a set of cuts on the different discriminators, the efficiency is shown as a function of proportion of nonprompt muons passing the WP selection.

The systematic uncertainties in the efficiencies estimated using the tag-and-probe method are smaller than 1% [2] and are correlated between the different discriminators.

The systematic uncertainties in the background contamination are strongly dependent on the topology of the background that contaminates each specific analysis; in particular, when the background contamination is due to muons with very different topology (e.g. multijet events) with respect to those of the signal region. For the prompt-muon MVA, which uses b tagging and other variables strongly dependent on the event topology, the uncertainties can be larger. However, no large dependences on the event topology have been observed at analysis level [3]. In either case, the analyses making use of these MVA selections should tailor the systematic uncertainty in their specific cases.

Several analyses in CMS have already used the prompt-muon MVA discriminator with an equivalent training to that described in this paper.

Some examples include the evidence of $\mathrm{t\bar{t}H}$ production [3–5], in which the use of the prompt-muon MVA (including an equivalent training for electrons) leads to a reduction in the nonprompt-lepton background from $\mathrm{t\bar{t}}$ events by a factor of 4 with respect to the use of an equivalent cut-based technique. A second example is the measurement of the WZ process [7, 8], or the multiboson production at $\sqrt{s} = 5.02$ TeV [6], where the use of this identification signficantly reduced the poorly modelled nonprompt-lepton background arising from Z + jets and $\mathrm{t\bar{t}}$ events. A third example is the search for electroweak production of supersymmetric particles [9] where the use of this discriminator improved the nonprompt-lepton background rejection, therefore limiting the associated systematic uncertainties. Finally, an alternative training of this discriminator was also employed in the observation of tZq production [46] and four top quark production ($\mathrm{t\bar{t}t\bar{t}}$) [10], as well as in other precision top quark measurements [47–49].

The muon MVA ID was not previously used in any CMS analysis, but it offers an alternative discriminator that could be used for high-efficiency WPs. In addition, it features a weaker dependence

2024 JINST 19 P02031

on the number of PU vertices compared with the standard cut-based approaches, which may be useful in the context of changing data-taking conditions or high PU scenarios expected in Run 3. These points are of particular interest for those precision analyses that are not statistically limited, such as the top quark or the electroweak precision measurements, allowing for a nearly background-free signal region. In addition to reducing the amount of background, this may significantly reduce also its associated systematic uncertainties.

6.1 Muon MVA ID performance

The efficiency for each of the WPs is measured in both data and DY simulation using the tag-and-probe method. The background contamination and the signal purity are measured in a $\mathrm{t\bar{t}}$ simulated sample that was not used for training. The background contamination is defined as the number of background muons passing the identification criteria divided by the total number of background muons that also fulfill the cut-based loose identification criteria, and the purity is calculated as the number of signal muons divided by the total number of muons, for all these muons passing the identification criteria. A slight improvement of the purity for muons with p_{T} between 10 and 20 GeV is observed when using the MVA discriminators, whereas purity values for higher p_{T} are similar to that of the cut-based ID.

The measured efficiencies as functions of p_{T} for the medium and tight WPs are shown in figure 7 in two η regions. The efficiency of the medium MVA ID is higher than 99.5%, and about 0.5% higher than the one achieved by the cut-based ID for a similar background contamination of around 50%. For the tight MVA ID WP, it achieves a 10% smaller background contamination than the medium MVA ID, and the efficiency is about 99% for muons with $p_{\mathrm{T}} > 30$ GeV and 1–2% smaller for muons with p_{T} between 10 and 30 GeV. Efficiencies in the p_{T} region between 120 and 200 GeV are evaluated using DY simulation and they are compatible with the ones in the 80 to 120 GeV region, but they show an increase in the uncertainty of approximately a factor 2. Figure 8 shows the efficiency as a function of the number of vertices for both WPs. It remains around 99.5 (98.0)% for the medium (tight) muon MVA ID WP even for events with up to 60 PU vertices. For the medium WP of the cut-based ID, the efficiency decreases as a function of the number of PU vertices, whereas it is stable for the medium WP of the muon MVA ID. The efficiency in DY simulation is systematically 0.5–1.0% higher than the efficiency in data as a result of small imperfections in the modelling. The discrepancy is observed both in the cut-based ID, as reported in ref. [2], and in the muon MVA ID.

6.2 Prompt-muon MVA performance

The efficiency of the selected WP (prompt-muon MVA > 0.85) is measured both in data and DY simulation as a function of the muon p_{T} in two η regions using the tag-and-probe method, as in the previous section.

The measured efficiencies are shown in figure 9. Efficiencies are above 80% for muons with $p_{\mathrm{T}} > 20$ GeV. The efficiency is modelled well by simulations, with discrepancies smaller than 3% for muons with $p_{\mathrm{T}} > 20$ GeV. Efficiencies in the p_{T} region between 120 and 200 GeV are evaluated using $\mathrm{t\bar{t}}$ simulation and are compatible with the values in the 80 to 120 GeV region.

The rate of nonprompt muons is measured in a sample enriched in multijet events. This sample is obtained selecting data collected with a set of prescaled single muon triggers that do not require

2024 JINST 19 P02031

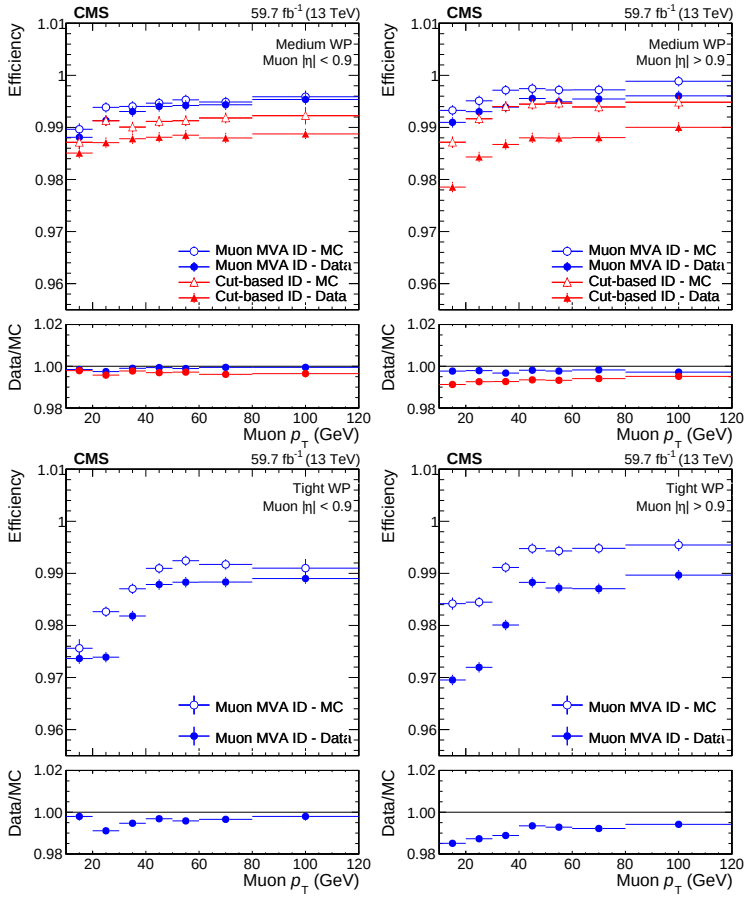


Figure 7. Muon identification efficiency for the medium (upper) and tight (lower) WPs as a function of p_T for muons with $|\eta| < 0.9$ (left) and $|\eta| > 0.9$ (right). Blue dots show the muon MVA ID performance both for the 2018 data set and DY simulation, whereas red triangles show the efficiency of the medium cut-based ID used during Run 2. The data to MC ratio is also shown. The efficiencies of the muon MVA ID are similar in both η regions.

isolation. The same trigger selection is applied to the simulated events. Events are required to have a muon passing the minimal muon selection described in section 5. Additionally, to suppress the contribution from light-flavour meson decays, muons are required to fulfill the medium cut-based requirements. Moreover, events are required to have a jet with $p_T > 30$ GeV and $|\eta| < 2.4$ recoiling against a muon with a ΔR between the jet and the muon of less than 0.7. Figure 10 shows a set of the most important variables for events passing this selection. The multijet background enriched region defined above is dominated by nonprompt muons mostly coming from heavy-flavour hadron decays. In general, the input variables of the prompt-muon MVA, as well as the MVA score, are modelled quite well by simulation. An exception to this is the segment compatibility variable, which shows a clear disagreement at lower values. This is due to the fact that simulated multijet events are filtered, so they contain a muon produced at the PV, and they do not include a significant part of the PU contribution because only events with a muon in the hard scattering are selected. These muons are typically not relevant for the analyses, since they are easily rejected by the preselection requirements. The p_T distribution is also not well modelled in these background samples, because

2024 JINST 19 P02031

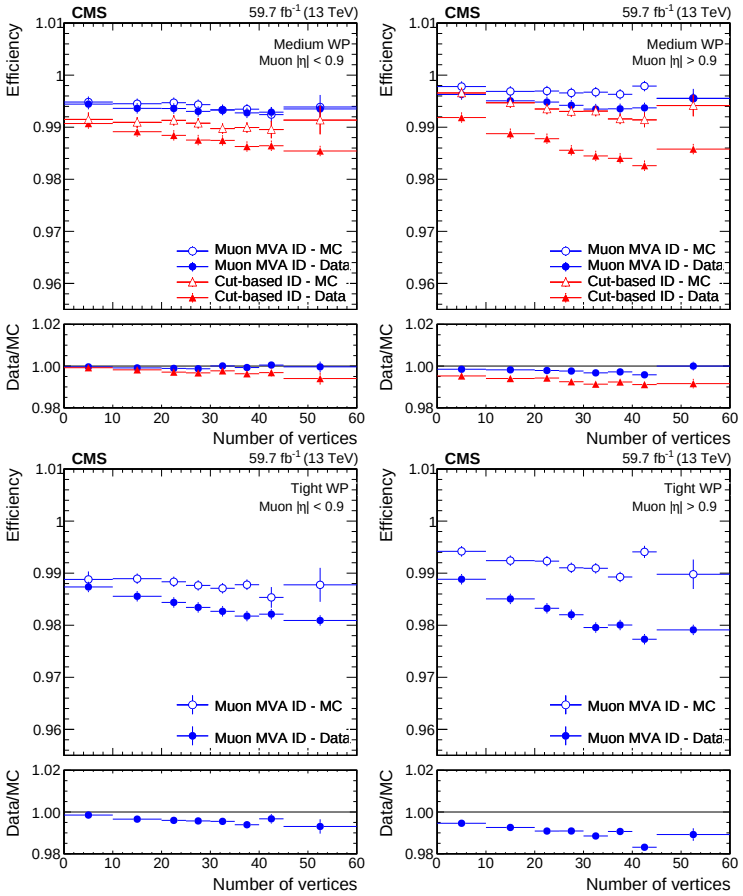


Figure 8. Muon identification efficiency for the medium (upper) and tight (lower) WPs as a function of PU for muons with $|\eta| < 0.9$ (left) and $|\eta| > 0.9$ (right). Blue dots show the muon MVA ID performance both for the 2018 data set and DY simulation, whereas red triangles show the efficiency of the medium cut-based ID used during Run 2. The data to MC ratio is also shown.

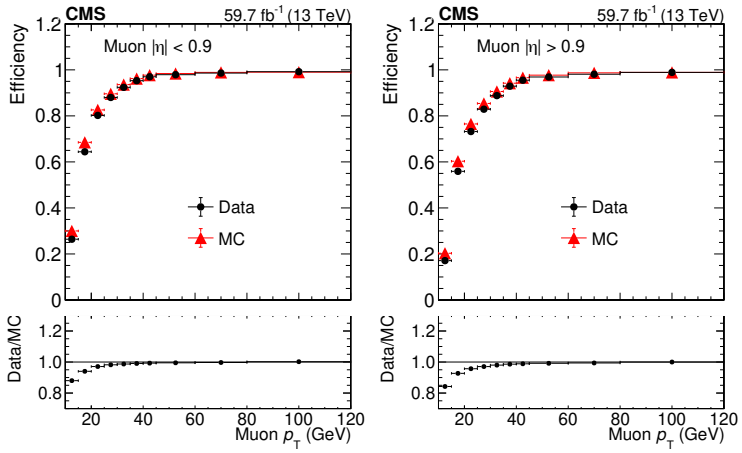


Figure 9. Efficiency of the prompt-muon MVA selection as a function of the muon p_{T} for muons with $|\eta| < 0.9$ (left) and $|\eta| > 0.9$ (right), for the 2018 data set with black dots and simulated DY events with red triangles. The vertical bars on the plots represent the statistical uncertainty of each measurement.

2024 JINST 19 P02031

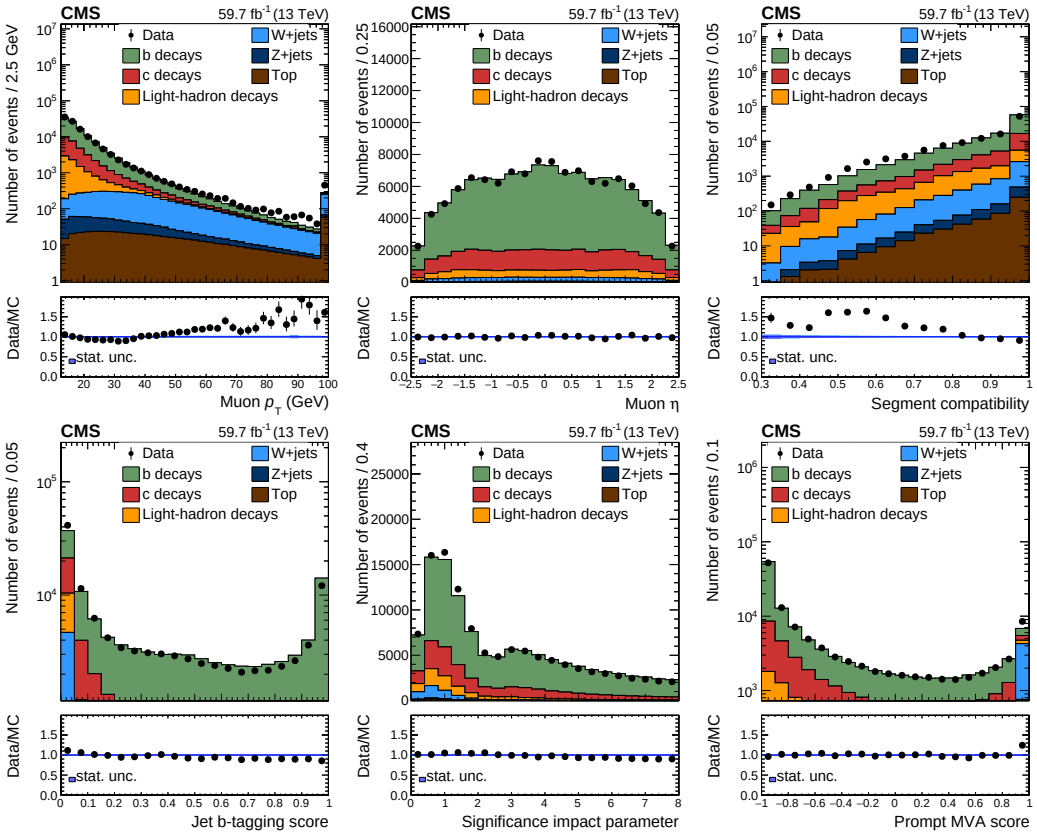


Figure 10. Distribution of data in the multijet control region as a function of the muon p_T (upper left), η (upper central), segment compatibility (upper right), the DeepJet b tagging score of the jet associated to the muon (lower left), the significance of the impact parameter (lower central) and the prompt-muon MVA score (lower right). The vertical bars on the dots represent the statistical uncertainty of each data point and the blue band, the uncertainty associated to the limited number of simulated events.

the employed multijet samples have a limited accuracy. However, the amount of mismodelling is small in the signal and background samples used in the training.

The sample defined by the selection described above is enriched in nonprompt muons. However, background contributions may arise from electroweak-induced processes such as W + jets or $t\bar{t}$ events. To subtract this component, the observable m_T^{fix} is defined as:

$$m_T^{fix} = \sqrt{2 p_T^{fix} p_T^{miss} (1 - \cos\Delta\phi)}, \tag{6.1}$$

where $\Delta\phi$ is the azhimutal angle between the muon and $\vec{p}_T^{miss}$. The definition of m_T^{fix} is similar to that of the transverse mass of the muon and p_T^{miss}; the only difference is that the muon momentum is set to $p_T^{fix} = 35\,\text{GeV}$, approximately the mode of the muon p_T distribution in W + jets events. Similarly to the transverse mass, the m_T^{fix} variable has a kinematic endpoint near the W boson mass. However, since the muon p_T is not included in this calculation, it is less correlated with this quantity, avoiding potential biases in the measurement.

Then, the number of events with a nonprompt muon is computed by means of a fit to the m_T^{fix} observable. In the fit, the prompt and nonprompt contributions are parameterized using templates

2024 JINST 19 P02031

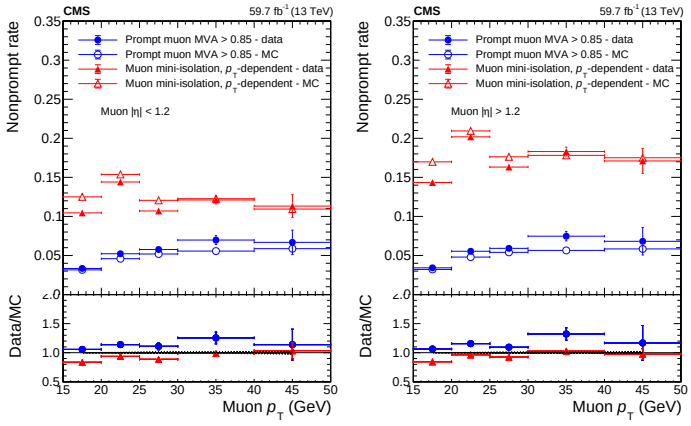


Figure 11. Measurement of the nonprompt-muon rate of a prompt-muon MVA (blue dots) and mini-isolation (red triangles) selection as a function of p_T for muons with $|\eta| < 1.2$ (left) and $|\eta| > 1.2$ (right) for the 2018 data set and simulated DY events.

that are derived from samples of simulated events of each muon source. The prompt contribution is obtained from W + jets, DY+jets, and $t\bar{t}$ simulated events, whereas the nonprompt contribution includes multijet events with muons in the final state. The fit also incorporates nuisance parameters to account for statistical uncertainties in the templates, as well as systematic deformations of their shapes. The fit is performed separately for cases in which the muon passes or fails a prompt-muon MVA score larger than 0.85. We label the result of each of the two fits as N_{pass} and N_{fail}, respectively, and the nonprompt rate, f, is computed as

$$f = \frac{N_{\text{pass}}}{N_{\text{pass}} + N_{\text{fail}}}. \tag{6.2}$$

Additionally, to compare the performance of the prompt-muon MVA with a more standard criterion designed to reject $t\bar{t}$ events, the nonprompt-muon rate with a selection based on mini-isolation is also computed. Since the prompt-muon MVA and the mini-isolation have a different efficiency dependence as a function of the muon p_T, a requirement on mini-isolation, which is dependent on p_T, is included that gives the same efficiency as the prompt-muon MVA and thus provides a fair comparison.

The nonprompt-muon rates for the two selections are shown in figure 11, displaying approximately a factor 2 (3) smaller nonprompt rate of the prompt-muon MVA with respect to the mini-isolation selection for muons with $|\eta| < 1.2$ (> 1.2). Additionally, the observed nonprompt rate agrees with the predictions provided by the simulations, which also reproduces the difference in nonprompt rate between the two strategies. This result validates the prompt-muon MVA in collision data and also shows its generalization power in a phase space different from the one used for its training.

7 Summary

A correct identification of the leptons is crucial in many precision measurements and searches to suppress the otherwise overwhelming background and as an indicator of interesting physical processes. Two multivariate analyses were developed for highly efficient muon identification and isolation. The first one, the muon MVA ID, is trained to distinguish muons produced promptly in

2024 JINST 19 P02031

heavy gauge boson decays as well as muons from τ lepton and heavy-flavour hadron decays, from background muons produced in light-hadron decays (pions or kaons) or other spurious signatures in the detector that could be misreconstructed as muons. The discriminator is presented as an alternative to the standard cut-based identification criteria and could be used for high-efficiency working points. The second one, the prompt-muon MVA, selects isolated muons from W, Z, Higgs bosons, and τ lepton decays to reduce the contamination from nonisolated muons arising in heavy-flavour hadron decays. Their performances are measured in proton-proton collisions recorded by the CMS experiment during 2018 and compared to simulation. The performance of the muon MVA ID improves significantly that of the cut-based ID and the prompt-muon MVA achieves a factor 2–3 times smaller nonprompt-muon rates than the mini-isolation selection.

Acknowledgments

We congratulate our colleagues in the CERN accelerator departments for the excellent performance of the LHC and thank the technical and administrative staffs at CERN and at other CMS institutes for their contributions to the success of the CMS effort. In addition, we gratefully acknowledge the computing centres and personnel of the Worldwide LHC Computing Grid and other centres for delivering so effectively the computing infrastructure essential to our analyses. Finally, we acknowledge the enduring support for the construction and operation of the LHC, the CMS detector, and the supporting computing infrastructure provided by the following funding agencies: SC (Armenia), BMBWF and FWF (Austria); FNRS and FWO (Belgium); CNPq, CAPES, FAPERJ, FAPERGS, and FAPESP (Brazil); MES and BNSF (Bulgaria); CERN; CAS, MoST, and NSFC (China); MINCIENCIAS (Colombia); MSES and CSF (Croatia); RIF (Cyprus); SENESCYT (Ecuador); MoER, ERC PUT and ERDF (Estonia); Academy of Finland, MEC, and HIP (Finland); CEA and CNRS/IN2P3 (France); SRNSF (Georgia); BMBF, DFG, and HGF (Germany); GSRI (Greece); NKFIH (Hungary); DAE and DST (India); IPM (Iran); SFI (Ireland); INFN (Italy); MSIP and NRF (Republic of Korea); MES (Latvia); LAS (Lithuania); MOE and UM (Malaysia); BUAP, CINVESTAV, CONACYT, LNS, SEP, and UASLP-FAI (Mexico); MOS (Montenegro); MBIE (New Zealand); PAEC (Pakistan); MES and NSC (Poland); FCT (Portugal); MESTD (Serbia); MCIN/AEI and PCTI (Spain); MOSTR (Sri Lanka); Swiss Funding Agencies (Switzerland); MST (Taipei); MHESI and NSTDA (Thailand); TUBITAK and TENMAK (Turkey); NASU (Ukraine); STFC (United Kingdom); DOE and NSF (U.S.A.).

Individuals have received support from the Marie-Curie programme and the European Research Council and Horizon 2020 Grant, contract Nos. 675440, 724704, 752730, 758316, 765710, 824093, and COST Action CA16108 (European Union); the Leventis Foundation; the Alfred P. Sloan Foundation; the Alexander von Humboldt Foundation; the Science Committee, project no. 22rl-037 (Armenia); the Belgian Federal Science Policy Office; the Fonds pour la Formation à la Recherche dans l'Industrie et dans l'Agriculture (FRIA-Belgium); the Agentschap voor Innovatie door Wetenschap en Technologie (IWT-Belgium); the F.R.S.-FNRS and FWO (Belgium) under the "Excellence of Science — EOS" — be.h project n. 30820817; the Beijing Municipal Science & Technology Commission, No. Z191100007219010 and Fundamental Research Funds for the Central Universities (China); the Ministry of Education, Youth and Sports (MEYS) of the Czech Republic; the Shota Rustaveli National Science Foundation, grant FR-22-985 (Georgia); the Deutsche Forschungsgemeinschaft (DFG), under Germany's Excellence Strategy — EXC 2121 "Quantum

2024 JINST 19 P02031

Universe" — 390833306, and under project number 400140256 - GRK2497; the Hellenic Foundation for Research and Innovation (HFRI), Project Number 2288 (Greece); the Hungarian Academy of Sciences, the New National Excellence Program - ÚNKP, the NKFIH research grants K 124845, K 124850, K 128713, K 128786, K 129058, K 131991, K 133046, K 138136, K 143460, K 143477, 2020-2.2.1-ED-2021-00181, and TKP2021-NKTA-64 (Hungary); the Council of Science and Industrial Research, India; ICSC — National Research Centre for High Performance Computing, Big Data and Quantum Computing, funded by the EU NexGeneration program (Italy); the Latvian Council of Science; the Ministry of Education and Science, project no. 2022/WK/14, and the National Science Center, contracts Opus 2021/41/B/ST2/01369 and 2021/43/B/ST2/01552 (Poland); the Fundação para a Ciência e a Tecnologia, grant CEECIND/01334/2018 (Portugal); the National Priorities Research Program by Qatar National Research Fund; MCIN/AEI/10.13039/501100011033, ERDF "a way of making Europe", and the Programa Estatal de Fomento de la Investigación Científica y Técnica de Excelencia María de Maeztu, grant MDM-2017-0765 and Programa Severo Ochoa del Principado de Asturias (Spain); the Chulalongkorn Academic into Its 2nd Century Project Advancement Project, and the National Science, Research and Innovation Fund via the Program Management Unit for Human Resources & Institutional Development, Research and Innovation, grant B05F650021 (Thailand); the Kavli Foundation; the Nvidia Corporation; the SuperMicro Corporation; the Welch Foundation, contract C-1845; and the Weston Havens Foundation (U.S.A.).

References

[1] CMS collaboration, *The CMS Experiment at the CERN LHC*, 2008 *JINST* **3** S08004.

[2] CMS collaboration, *Performance of the CMS muon detector and muon reconstruction with proton-proton collisions at* $\sqrt{s} = 13$ *TeV*, 2018 *JINST* **13** P06015 [arXiv:1804.04528].

[3] CMS collaboration, *Measurement of the Higgs boson production rate in association with top quarks in final states with electrons, muons, and hadronically decaying tau leptons at* $\sqrt{s} = 13$ *TeV*, *Eur. Phys. J. C* **81** (2021) 378 [arXiv:2011.03652].

[4] CMS collaboration, *Evidence for associated production of a Higgs boson with a top quark pair in final states with electrons, muons, and hadronically decaying* τ *leptons at* $\sqrt{s} = 13$ *TeV*, *JHEP* **08** (2018) 066 [arXiv:1803.05485].

[5] CMS collaboration, *Observation of* $\mathrm{t\bar{t}}H$ *production*, *Phys. Rev. Lett.* **120** (2018) 231801 [arXiv:1804.02610].

[6] CMS collaboration, *Measurements of the electroweak diboson production cross sections in proton-proton collisions at* $\sqrt{s} = 5.02$ *TeV using leptonic decays*, *Phys. Rev. Lett.* **127** (2021) 191801 [arXiv:2107.01137].

[7] CMS collaboration, *Measurement of the inclusive and differential WZ production cross sections, polarization angles, and triple gauge couplings in pp collisions at* $\sqrt{s}13$ *TeV*, *JHEP* **07** (2022) 032 [arXiv:2110.11231].

[8] CMS collaboration, *Measurements of the* $pp \to WZ$ *inclusive and differential production cross section and constraints on charged anomalous triple gauge couplings at* $\sqrt{s} = 13$ *TeV*, *JHEP* **04** (2019) 122 [arXiv:1901.03428].

[9] CMS collaboration, *Search for electroweak production of charginos and neutralinos in proton-proton collisions at* $\sqrt{s} = 13$ *TeV*, *JHEP* **04** (2022) 147 [arXiv:2106.14246].

2024 JINST 19 P02031

[10] CMS collaboration, *Observation of four top quark production in proton-proton collisions at* $\sqrt{s} = 13$ *TeV*, *Phys. Lett. B* **847** (2023) 138290 [arXiv:2305.13439].

[11] CMS collaboration, *Measurement of properties of* $B_s^0 \to \mu^+\mu^-$ *decays and search for* $B^0 \to \mu^+\mu^-$ *with the CMS experiment*, *JHEP* **04** (2020) 188 [arXiv:1910.12127].

[12] CMS collaboration, *Performance of the CMS Level-1 trigger in proton-proton collisions at* $\sqrt{s} = 13$ *TeV*, 2020 *JINST* **15** P10017 [arXiv:2006.10165].

[13] CMS collaboration, *The CMS trigger system*, 2017 *JINST* **12** P01020 [arXiv:1609.02366].

[14] CMS collaboration, *CMS luminosity measurement for the 2018 data-taking period at* $\sqrt{s} = 13$ *TeV*, Tech. Rep. CMS-PAS-LUM-18-002, CERN, Geneva (2019).

[15] CMS collaboration, *Precision luminosity measurement in proton-proton collisions at* $\sqrt{s} = 13$ *TeV in 2015 and 2016 at CMS*, *Eur. Phys. J. C* **81** (2021) 800 [arXiv:2104.01927].

[16] CMS collaboration, *Performance of the CMS muon trigger system in proton-proton collisions at* $\sqrt{s} = 13$ *TeV*, 2021 *JINST* **16** P07001 [arXiv:2102.04790].

[17] J. Alwall et al., *The automated computation of tree-level and next-to-leading order differential cross sections, and their matching to parton shower simulations*, *JHEP* **07** (2014) 079 [arXiv:1405.0301].

[18] J. Alwall et al., *Comparative study of various algorithms for the merging of parton showers and matrix elements in hadronic collisions*, *Eur. Phys. J. C* **53** (2008) 473 [arXiv:0706.2569].

[19] S. Alioli, P. Nason, C. Oleari and E. Re, *A general framework for implementing NLO calculations in shower Monte Carlo programs: the POWHEG BOX*, *JHEP* **06** (2010) 043 [arXiv:1002.2581].

[20] S. Frixione, P. Nason and C. Oleari, *Matching NLO QCD computations with Parton Shower simulations: the POWHEG method*, *JHEP* **11** (2007) 070 [arXiv:0709.2092].

[21] P. Nason, *A New method for combining NLO QCD with shower Monte Carlo algorithms*, *JHEP* **11** (2004) 040 [hep-ph/0409146].

[22] NNPDF collaboration, *Parton distributions from high-precision collider data*, *Eur. Phys. J. C* **77** (2017) 663 [arXiv:1706.00428].

[23] T. Sjöstrand et al., *An introduction to PYTHIA 8.2*, *Comput. Phys. Commun.* **191** (2015) 159 [arXiv:1410.3012].

[24] P. Skands, S. Carrazza and J. Rojo, *Tuning PYTHIA 8.1: the Monash 2013 Tune*, *Eur. Phys. J. C* **74** (2014) 3024 [arXiv:1404.5630].

[25] CMS collaboration, *Extraction and validation of a new set of CMS PYTHIA8 tunes from underlying-event measurements*, *Eur. Phys. J. C* **80** (2020) 4 [arXiv:1903.12179].

[26] R. Frederix and S. Frixione, *Merging meets matching in MC@NLO*, *JHEP* **12** (2012) 061 [arXiv:1209.6215].

[27] GEANT4 collaboration, *GEANT4–a simulation toolkit*, *Nucl. Instrum. Meth. A* **506** (2003) 250.

[28] R. Fruhwirth, *Application of Kalman filtering to track and vertex fitting*, *Nucl. Instrum. Meth. A* **262** (1987) 444.

[29] CMS collaboration, *Description and performance of track and primary-vertex reconstruction with the CMS tracker*, 2014 *JINST* **9** P10009 [arXiv:1405.6569].

[30] CMS collaboration, *Performance of the reconstruction and identification of high-momentum muons in proton-proton collisions at* $\sqrt{s} = 13$ *TeV*, 2020 *JINST* **15** P02027 [arXiv:1912.03516].

2024 JINST 19 P02031

[31] D. Contardo et al., *Technical Proposal for the Phase-II Upgrade of the CMS Detector*, Tech. Rep. CERN-LHCC-2015-010 CERN, Geneva (2015) [DOI:10.17181/CERN.VU8I.D59J].

[32] CMS collaboration, *Particle-flow reconstruction and global event description with the CMS detector*, 2017 *JINST* **12** P10003 [arXiv:1706.04965].

[33] M. Cacciari, G.P. Salam and G. Soyez, *The anti-k_t jet clustering algorithm*, *JHEP* **04** (2008) 063 [arXiv:0802.1189].

[34] M. Cacciari, G.P. Salam and G. Soyez, *FastJet User Manual*, *Eur. Phys. J. C* **72** (2012) 1896 [arXiv:1111.6097].

[35] M. Cacciari, G.P. Salam and G. Soyez, *The Catchment Area of Jets*, *JHEP* **04** (2008) 005 [arXiv:0802.1188].

[36] M. Cacciari and G.P. Salam, *Pileup subtraction using jet areas*, *Phys. Lett. B* **659** (2008) 119 [arXiv:0707.1378].

[37] CMS collaboration, *Jet energy scale and resolution in the CMS experiment in pp collisions at* 8 *TeV*, 2017 *JINST* **12** P02014 [arXiv:1607.03663].

[38] CMS collaboration, *Performance summary of AK4 jet b tagging with data from proton-proton collisions at* 13 *TeV with the CMS detector*, Tech. Rep. CMS-DP-2023-005 CERN, Geneva (2023).

[39] E. Bols et al., *Jet Flavour Classification Using DeepJet*, 2020 *JINST* **15** P12012 [arXiv:2008.10519].

[40] CMS collaboration, *Performance of Electron Reconstruction and Selection with the CMS Detector in Proton-Proton Collisions at* $\sqrt{s} = 8$ *TeV*, 2015 *JINST* **10** P06005 [arXiv:1502.02701].

[41] CMS collaboration, *Search for supersymmetry in pp collisions at* $\sqrt{s} = 13$ *TeV in the single-lepton final state using the sum of masses of large-radius jets*, *JHEP* **08** (2016) 122 [arXiv:1605.04608].

[42] A. Prinzie and D.V. den Poel, *Random Multiclass Classification: Generalizing Random Forests to Random MNL and Random NB*, in *Lecture Notes in Computer Science*, Springer Berlin Heidelberg (2007), p. 349–358 [DOI:10.1007/978-3-540-74469-6_35].

[43] F. Pedregosa et al., *Scikit-learn: Machine Learning in Python*, *J. Machine Learning Res.* **12** (2011) 2825 [arXiv:1201.0490].

[44] H. Voss, A. Hocker, J. Stelzer and F. Tegenfeldt, *TMVA, the Toolkit for Multivariate Data Analysis with ROOT*, *PoS* **ACAT** (2007) 040 [physics/0703039].

[45] CMS collaboration, *Measurements of Inclusive W and Z Cross Sections in pp Collisions at* $\sqrt{s} = 7$ *TeV*, *JHEP* **01** (2011) 080 [arXiv:1012.2466].

[46] CMS collaboration, *Observation of Single Top Quark Production in Association with a Z Boson in Proton-Proton Collisions at* $\sqrt{s} = 13$ *TeV*, *Phys. Rev. Lett.* **122** (2019) 132003 [arXiv:1812.05900].

[47] CMS collaboration, *Measurement of the cross section of top quark-antiquark pair production in association with a W boson in proton-proton collisions at* $\sqrt{s} = 13$ *TeV*, *JHEP* **07** (2023) 219 [arXiv:2208.06485].

[48] CMS collaboration, *Measurement of top quark pair production in association with a Z boson in proton-proton collisions at* $\sqrt{s} = 13$ *TeV*, *JHEP* **03** (2020) 056 [arXiv:1907.11270].

[49] CMS collaboration, *Inclusive and differential cross section measurements of single top quark production in association with a Z boson in proton-proton collisions at* $\sqrt{s} = 13$ *TeV*, *JHEP* **02** (2022) 107 [arXiv:2111.02860].

2024 JINST 19 P02031

The CMS collaboration

Yerevan Physics Institute, Yerevan, Armenia

A. Hayrapetyan, A. Tumasyan[1]

Institut für Hochenergiephysik, Vienna, Austria

W. Adam, J.W. Andrejkovic, T. Bergauer, S. Chatterjee, K. Damanakis, M. Dragicevic, A. Escalante Del Valle, P.S. Hussain, M. Jeitler[2], N. Krammer, D. Liko, I. Mikulec, J. Schieck[2], R. Schöfbeck, D. Schwarz, M. Sonawane, S. Templ, W. Waltenberger, C.-E. Wulz[2]

Universiteit Antwerpen, Antwerpen, Belgium

M.R. Darwish[3], T. Janssen, P. Van Mechelen

Vrije Universiteit Brussel, Brussel, Belgium

E.S. Bols, J. D'Hondt, S. Dansana, A. De Moor, M. Delcourt, H. El Faham, S. Lowette, I. Makarenko, D. Müller, A.R. Sahasransu, S. Tavernier, M. Tytgat[4], S. Van Putte, D. Vannerom

Université Libre de Bruxelles, Bruxelles, Belgium

B. Clerbaux, G. De Lentdecker, L. Favart, D. Hohov, J. Jaramillo, A. Khalilzadeh, K. Lee, M. Mahdavikhorrami, A. Malara, S. Paredes, L. Pétré, N. Postiau, L. Thomas, M. Vanden Bemden, C. Vander Velde, P. Vanlaer

Ghent University, Ghent, Belgium

M. De Coen, D. Dobur, Y. Hong, J. Knolle, L. Lambrecht, G. Mestdach, C. Rendón, A. Samalan, K. Skovpen, N. Van Den Bossche, L. Wezenbeek

Université Catholique de Louvain, Louvain-la-Neuve, Belgium

A. Benecke, G. Bruno, C. Caputo, C. Delaere, I.S. Donertas, A. Giammanco, K. Jaffel, Sa. Jain, V. Lemaitre, J. Lidrych, P. Mastrapasqua, K. Mondal, T.T. Tran, S. Wertz

Centro Brasileiro de Pesquisas Fisicas, Rio de Janeiro, Brazil

G.A. Alves, E. Coelho, C. Hensel, T. Menezes De Oliveira, A. Moraes, P. Rebello Teles, M. Soeiro

Universidade do Estado do Rio de Janeiro, Rio de Janeiro, Brazil

W.L. Aldá Júnior, M. Alves Gallo Pereira, M. Barroso Ferreira Filho, H. Brandao Malbouisson, W. Carvalho, J. Chinellato[5], E.M. Da Costa, G.G. Da Silveira[6], D. De Jesus Damiao, S. Fonseca De Souza, J. Martins[7], C. Mora Herrera, K. Mota Amarilo, L. Mundim, H. Nogima, A. Santoro, S.M. Silva Do Amaral, A. Sznajder, M. Thiel, A. Vilela Pereira

Universidade Estadual Paulista, Universidade Federal do ABC, São Paulo, Brazil

C.A. Bernardes[6], L. Calligaris, T.R. Fernandez Perez Tomei, E.M. Gregores, P.G. Mercadante, S.F. Novaes, B. Orzari, Sandra S. Padula

2024 JINST 19 P02031

Institute for Nuclear Research and Nuclear Energy, Bulgarian Academy of Sciences, Sofia, Bulgaria
A. Aleksandrov, G. Antchev, R. Hadjiiska, P. Iaydjiev, M. Misheva, M. Shopova, G. Sultanov

University of Sofia, Sofia, Bulgaria
A. Dimitrov, T. Ivanov, L. Litov, B. Pavlov, P. Petkov, A. Petrov, E. Shumka

Instituto De Alta Investigación, Universidad de Tarapacá, Casilla 7 D, Arica, Chile
S. Keshri, S. Thakur

Beihang University, Beijing, China
T. Cheng, Q. Guo, T. Javaid, M. Mittal, L. Yuan

Department of Physics, Tsinghua University, Beijing, China
G. Bauer[8,9], Z. Hu, K. Yi[8,10]

Institute of High Energy Physics, Beijing, China
G.M. Chen[11], H.S. Chen[11], M. Chen[11], F. Iemmi, C.H. Jiang, A. Kapoor[12], H. Liao, Z.-A. Liu[13], F. Monti, M.A. Shahzad[11], R. Sharma[14], J.N. Song[13], J. Tao, C. Wang[11], J. Wang, Z. Wang[11], H. Zhang

State Key Laboratory of Nuclear Physics and Technology, Peking University, Beijing, China
A. Agapitos, Y. Ban, A. Levin, C. Li, Q. Li, Y. Mao, S.J. Qian, X. Sun, D. Wang, H. Yang, C. Zhou

Sun Yat-Sen University, Guangzhou, China
Z. You

University of Science and Technology of China, Hefei, China
N. Lu

Institute of Modern Physics and Key Laboratory of Nuclear Physics and Ion-beam Application (MOE) — Fudan University, Shanghai, China
X. Gao[15], D. Leggat, H. Okawa, Y. Zhang

Zhejiang University, Hangzhou, Zhejiang, China
Z. Lin, C. Lu, M. Xiao

Universidad de Los Andes, Bogota, Colombia
C. Avila, D.A. Barbosa Trujillo, A. Cabrera, C. Florez, J. Fraga, J.A. Reyes Vega

Universidad de Antioquia, Medellin, Colombia
J. Mejia Guisao, F. Ramirez, M. Rodriguez, J.D. Ruiz Alvarez

2024 JINST 19 P02031

University of Split, Faculty of Electrical Engineering, Mechanical Engineering and Naval Architecture, Split, Croatia
D. Giljanovic, N. Godinovic, D. Lelas, A. Sculac

University of Split, Faculty of Science, Split, Croatia
M. Kovac, T. Sculac

Institute Rudjer Boskovic, Zagreb, Croatia
P. Bargassa, V. Brigljevic, B.K. Chitroda, D. Ferencek, S. Mishra, A. Starodumov[16], T. Susa

University of Cyprus, Nicosia, Cyprus
A. Attikis, K. Christoforou, S. Konstantinou, J. Mousa, C. Nicolaou, F. Ptochos, P.A. Razis, H. Rykaczewski, H. Saka, A. Stepennov

Charles University, Prague, Czech Republic
M. Finger, M. Finger Jr., A. Kveton

Escuela Politecnica Nacional, Quito, Ecuador
E. Ayala

Universidad San Francisco de Quito, Quito, Ecuador
E. Carrera Jarrin

Academy of Scientific Research and Technology of the Arab Republic of Egypt, Egyptian Network of High Energy Physics, Cairo, Egypt
H. Abdalla[17], Y. Assran[18,19]

Center for High Energy Physics (CHEP-FU), Fayoum University, El-Fayoum, Egypt
M.A. Mahmoud, Y. Mohammed

National Institute of Chemical Physics and Biophysics, Tallinn, Estonia
R.K. Dewanjee[20], K. Ehataht, M. Kadastik, T. Lange, S. Nandan, C. Nielsen, J. Pata, M. Raidal, L. Tani, C. Veelken

Department of Physics, University of Helsinki, Helsinki, Finland
H. Kirschenmann, K. Osterberg, M. Voutilainen

Helsinki Institute of Physics, Helsinki, Finland
S. Bharthuar, E. Brücken, F. Garcia, J. Havukainen, K.T.S. Kallonen, M.S. Kim, R. Kinnunen, T. Lampén, K. Lassila-Perini, S. Lehti, T. Lindén, M. Lotti, L. Martikainen, M. Myllymäki, M.m. Rantanen, H. Siikonen, E. Tuominen, J. Tuominiemi

Lappeenranta-Lahti University of Technology, Lappeenranta, Finland
P. Luukka, H. Petrow, T. Tuuva[†]

2024 JINST 19 P02031

IRFU, CEA, Université Paris-Saclay, Gif-sur-Yvette, France
M. Besancon, F. Couderc, M. Dejardin, D. Denegri, J.L. Faure, F. Ferri, S. Ganjour, P. Gras, G. Hamel de Monchenault, V. Lohezic, J. Malcles, J. Rander, A. Rosowsky, M.Ö. Sahin, A. Savoy-Navarro[21], P. Simkina, M. Titov

Laboratoire Leprince-Ringuet, CNRS/IN2P3, Ecole Polytechnique, Institut Polytechnique de Paris, Palaiseau, France
C. Baldenegro Barrera, F. Beaudette, A. Buchot Perraguin, P. Busson, A. Cappati, C. Charlot, F. Damas, O. Davignon, A. De Wit, G. Falmagne, B.A. Fontana Santos Alves, S. Ghosh, A. Gilbert, R. Granier de Cassagnac, A. Hakimi, B. Harikrishnan, L. Kalipoliti, G. Liu, J. Motta, M. Nguyen, C. Ochando, L. Portales, R. Salerno, U. Sarkar, J.B. Sauvan, Y. Sirois, A. Tarabini, E. Vernazza, A. Zabi, A. Zghiche

Université de Strasbourg, CNRS, IPHC UMR 7178, Strasbourg, France
J.-L. Agram[22], J. Andrea, D. Apparu, D. Bloch, J.-M. Brom, E.C. Chabert, C. Collard, S. Falke, U. Goerlach, C. Grimault, R. Haeberle, A.-C. Le Bihan, M.A. Sessini, P. Van Hove

Institut de Physique des 2 Infinis de Lyon (IP2I), Villeurbanne, France
S. Beauceron, B. Blancon, G. Boudoul, N. Chanon, J. Choi, D. Contardo, P. Depasse, C. Dozen[23], H. El Mamouni, J. Fay, S. Gascon, M. Gouzevitch, C. Greenberg, G. Grenier, B. Ille, I.B. Laktineh, M. Lethuillier, L. Mirabito, S. Perries, A. Purohit, M. Vander Donckt, P. Verdier, J. Xiao

Georgian Technical University, Tbilisi, Georgia
I. Bagaturia[24], I. Lomidze, Z. Tsamalaidze[16]

RWTH Aachen University, I. Physikalisches Institut, Aachen, Germany
V. Botta, L. Feld, K. Klein, M. Lipinski, D. Meuser, A. Pauls, N. Röwert, M. Teroerde

RWTH Aachen University, III. Physikalisches Institut A, Aachen, Germany
S. Diekmann, A. Dodonova, N. Eich, D. Eliseev, F. Engelke, M. Erdmann, P. Fackeldey, B. Fischer, T. Hebbeker, K. Hoepfner, F. Ivone, A. Jung, M.y. Lee, L. Mastrolorenzo, M. Merschmeyer, A. Meyer, S. Mukherjee, D. Noll, A. Novak, F. Nowotny, A. Pozdnyakov, Y. Rath, W. Redjeb, F. Rehm, H. Reithler, V. Sarkisovi, A. Schmidt, S.C. Schuler, A. Sharma, A. Stein, F. Torres Da Silva De Araujo[25], L. Vigilante, S. Wiedenbeck, S. Zaleski

RWTH Aachen University, III. Physikalisches Institut B, Aachen, Germany
C. Dziwok, G. Flügge, W. Haj Ahmad[26], T. Kress, A. Nowack, O. Pooth, A. Stahl, T. Ziemons, A. Zotz

Deutsches Elektronen-Synchrotron, Hamburg, Germany
H. Aarup Petersen, M. Aldaya Martin, J. Alimena, S. Amoroso, Y. An, S. Baxter, M. Bayatmakou, H. Becerril Gonzalez, O. Behnke, A. Belvedere, S. Bhattacharya, F. Blekman[27], K. Borras[28], D. Brunner, A. Campbell, A. Cardini, C. Cheng, F. Colombina, S. Consuegra Rodríguez, G. Correia Silva, M. De Silva, G. Eckerlin, D. Eckstein,

2024 JINST 19 P02031

L.I. Estevez Banos, O. Filatov, E. Gallo[27], A. Geiser, A. Giraldi, G. Greau, V. Guglielmi, M. Guthoff, A. Hinzmann, A. Jafari[29], L. Jeppe, N.Z. Jomhari, B. Kaech, M. Kasemann, H. Kaveh, C. Kleinwort, R. Kogler, M. Komm, D. Krücker, W. Lange, D. Leyva Pernia, K. Lipka[30], W. Lohmann[31], R. Mankel, I.-A. Melzer-Pellmann, M. Mendizabal Morentin, J. Metwally, A.B. Meyer, G. Milella, A. Mussgiller, A. Nürnberg, Y. Otarid, D. Pérez Adán, E. Ranken, A. Raspereza, B. Ribeiro Lopes, J. Rübenach, A. Saggio, M. Scham[32,28], S. Schnake[28], P. Schütze, C. Schwanenberger[27], D. Selivanova, M. Shchedrolosiev, R.E. Sosa Ricardo, L.P. Sreelatha Pramod, D. Stafford, F. Vazzoler, A. Ventura Barroso, R. Walsh, Q. Wang, Y. Wen, K. Wichmann, L. Wiens[28], C. Wissing, S. Wuchterl, Y. Yang, A. Zimermmane Castro Santos

University of Hamburg, Hamburg, Germany

A. Albrecht, S. Albrecht, M. Antonello, S. Bein, L. Benato, M. Bonanomi, P. Connor, M. Eich, K. El Morabit, Y. Fischer, A. Fröhlich, C. Garbers, E. Garutti, A. Grohsjean, M. Hajheidari, J. Haller, H.R. Jabusch, G. Kasieczka, P. Keicher, R. Klanner, W. Korcari, T. Kramer, V. Kutzner, F. Labe, J. Lange, A. Lobanov, C. Matthies, A. Mehta, L. Moureaux, M. Mrowietz, A. Nigamova, Y. Nissan, A. Paasch, K.J. Pena Rodriguez, T. Quadfasel, B. Raciti, M. Rieger, D. Savoiu, J. Schindler, P. Schleper, M. Schröder, J. Schwandt, M. Sommerhalder, H. Stadie, G. Steinbrück, A. Tews, M. Wolf

Karlsruher Institut fuer Technologie, Karlsruhe, Germany

S. Brommer, M. Burkart, E. Butz, T. Chwalek, A. Dierlamm, A. Droll, N. Faltermann, M. Giffels, A. Gottmann, F. Hartmann[33], R. Hofsaess, M. Horzela, U. Husemann, M. Klute, R. Koppenhöfer, M. Link, A. Lintuluoto, S. Maier, S. Mitra, M. Mormile, Th. Müller, M. Neukum, M. Oh, G. Quast, K. Rabbertz, B. Regnery, N. Shadskiy, I. Shvetsov, H.J. Simonis, N. Trevisani, R. Ulrich, J. van der Linden, R.F. Von Cube, M. Wassmer, S. Wieland, F. Wittig, R. Wolf, S. Wunsch, X. Zuo

Institute of Nuclear and Particle Physics (INPP), NCSR Demokritos, Aghia Paraskevi, Greece

G. Anagnostou, P. Assiouras, G. Daskalakis, A. Kyriakis, A. Papadopoulos[33], A. Stakia

National and Kapodistrian University of Athens, Athens, Greece

P. Kontaxakis, G. Melachroinos, A. Panagiotou, I. Papavergou, I. Paraskevas, N. Saoulidou, K. Theofilatos, E. Tziaferi, K. Vellidis, I. Zisopoulos

National Technical University of Athens, Athens, Greece

G. Bakas, T. Chatzistavrou, G. Karapostoli, K. Kousouris, I. Papakrivopoulos, E. Siamarkou, G. Tsipolitis, A. Zacharopoulou

University of Ioánnina, Ioánnina, Greece

K. Adamidis, I. Bestintzanos, I. Evangelou, C. Foudas, P. Gianneios, C. Kamtsikis, P. Katsoulis, P. Kokkas, P.G. Kosmoglou Kioseoglou, N. Manthos, I. Papadopoulos, J. Strologas

HUN-REN Wigner Research Centre for Physics, Budapest, Hungary

M. Bartók[34], C. Hajdu, D. Horvath[35,36], F. Sikler, V. Veszpremi

2024 JINST 19 P02031

MTA-ELTE Lendület CMS Particle and Nuclear Physics Group, Eötvös Loránd University, Budapest, Hungary

M. Csanád, K. Farkas, M.M.A. Gadallah[37], Á. Kadlecsik, P. Major, K. Mandal, G. Pásztor, A.J. Rádl[38], G.I. Veres

Faculty of Informatics, University of Debrecen, Debrecen, Hungary

P. Raics, B. Ujvari[39], G. Zilizi

Institute of Nuclear Research ATOMKI, Debrecen, Hungary

G. Bencze, S. Czellar, J. Karancsi[34], J. Molnar, Z. Szillasi

Karoly Robert Campus, MATE Institute of Technology, Gyongyos, Hungary

T. Csorgo[38], F. Nemes[38], T. Novak

Panjab University, Chandigarh, India

J. Babbar, S. Bansal, S.B. Beri, V. Bhatnagar, G. Chaudhary, S. Chauhan, N. Dhingra[40], R. Gupta, A. Kaur, A. Kaur, H. Kaur, M. Kaur, S. Kumar, M. Meena, K. Sandeep, T. Sheokand, J.B. Singh, A. Singla

University of Delhi, Delhi, India

A. Ahmed, A. Bhardwaj, A. Chhetri, B.C. Choudhary, A. Kumar, M. Naimuddin, K. Ranjan, S. Saumya

Saha Institute of Nuclear Physics, HBNI, Kolkata, India

S. Acharya[41], S. Baradia, S. Barman[42], S. Bhattacharya, D. Bhowmik, S. Dutta, S. Dutta, B. Gomber[41], P. Palit, G. Saha, B. Sahu[41], S. Sarkar

Indian Institute of Technology Madras, Madras, India

M.M. Ameen, P.K. Behera, S.C. Behera, S. Chatterjee, P. Jana, P. Kalbhor, J.R. Komaragiri[43], D. Kumar[43], L. Panwar[43], R. Pradhan, P.R. Pujahari, N.R. Saha, A. Sharma, A.K. Sikdar, S. Verma

Tata Institute of Fundamental Research-A, Mumbai, India

T. Aziz, I. Das, S. Dugad, M. Kumar, G.B. Mohanty, P. Suryadevara

Tata Institute of Fundamental Research-B, Mumbai, India

A. Bala, S. Banerjee, R.M. Chatterjee, M. Guchait, Sh. Jain, S. Karmakar, S. Kumar, G. Majumder, K. Mazumdar, S. Mukherjee, A. Thachayath

National Institute of Science Education and Research, An OCC of Homi Bhabha National Institute, Bhubaneswar, Odisha, India

S. Bahinipati[44], A.K. Das, C. Kar, D. Maity[45], P. Mal, T. Mishra, V.K. Muraleedharan Nair Bindhu[45], K. Naskar[45], A. Nayak[45], P. Sadangi, P. Saha, S.K. Swain, S. Varghese[45], D. Vats[45]

2024 JINST 19 P02031

Indian Institute of Science Education and Research (IISER), Pune, India
A. Alpana, S. Dube, B. Kansal, A. Laha, A. Rastogi, S. Sharma

Isfahan University of Technology, Isfahan, Iran
H. Bakhshiansohi[46], E. Khazaie[47], M. Zeinali[48]

Institute for Research in Fundamental Sciences (IPM), Tehran, Iran
S. Chenarani[49], S.M. Etesami, M. Khakzad, M. Mohammadi Najafabadi

University College Dublin, Dublin, Ireland
M. Grunewald

INFN Sezione di Bari[a], Università di Bari[b], Politecnico di Bari[c], Bari, Italy
M. Abbrescia[a,b], R. Aly[a,c,50], A. Colaleo[a,b], D. Creanza[a,c], B. D' Anzi[a,b], N. De Filippis[a,c], M. De Palma[a,b], A. Di Florio[a,c], W. Elmetenawee[a,b,50], L. Fiore[a], G. Iaselli[a,c], G. Maggi[a,c], M. Maggi[a], I. Margjeka[a,b], V. Mastrapasqua[a,b], S. My[a,b], S. Nuzzo[a,b], A. Pellecchia[a,b], A. Pompili[a,b], G. Pugliese[a,c], R. Radogna[a], G. Ramirez-Sanchez[a,c], D. Ramos[a], A. Ranieri[a], L. Silvestris[a], F.M. Simone[a,b], Ü. Sözbilir[a], A. Stamerra[a], R. Venditti[a], P. Verwilligen[a], A. Zaza[a,b]

INFN Sezione di Bologna[a], Università di Bologna[b], Bologna, Italy
G. Abbiendi[a], C. Battilana[a,b], D. Bonacorsi[a,b], L. Borgonovi[a], P. Capiluppi[a,b], A. Castro[a,b], F.R. Cavallo[a], M. Cuffiani[a,b], G.M. Dallavalle[a], T. Diotalevi[a,b], F. Fabbri[a], A. Fanfani[a,b], D. Fasanella[a,b], P. Giacomelli[a], L. Giommi[a,b], C. Grandi[a], L. Guiducci[a,b], S. Lo Meo[a,51], L. Lunerti[a,b], S. Marcellini[a], G. Masetti[a], F.L. Navarria[a,b], A. Perrotta[a], F. Primavera[a,b], A.M. Rossi[a,b], T. Rovelli[a,b], G.P. Siroli[a,b]

INFN Sezione di Catania[a], Università di Catania[b], Catania, Italy
S. Costa[a,b,52], A. Di Mattia[a], R. Potenza[a,b], A. Tricomi[a,b,52], C. Tuve[a,b]

INFN Sezione di Firenze[a], Università di Firenze[b], Firenze, Italy
G. Barbagli[a], G. Bardelli[a,b], B. Camaiani[a,b], A. Cassese[a], R. Ceccarelli[a], V. Ciulli[a,b], C. Civinini[a], R. D'Alessandro[a,b], E. Focardi[a,b], T. Kello[a], G. Latino[a,b], P. Lenzi[a,b], M. Lizzo[a], M. Meschini[a], S. Paoletti[a], A. Papanastassiou[a,b], G. Sguazzoni[a], L. Viliani[a]

INFN Laboratori Nazionali di Frascati, Frascati, Italy
L. Benussi, S. Bianco, R. Campagnola, M. Caponero[53], S. Meola[54], D. Piccolo, G. Saviano[55]

INFN Sezione di Genova[a], Università di Genova[b], Genova, Italy
P. Chatagnon[a], F. Ferro[a], E. Robutti[a], S. Tosi[a,b]

INFN Sezione di Milano-Bicocca[a], Università di Milano-Bicocca[b], Milano, Italy
A. Benaglia[a], G. Boldrini[a,b], F. Brivio[a], F. Cetorelli[a], F. De Guio[a,b], M.E. Dinardo[a,b], P. Dini[a], S. Gennai[a], A. Ghezzi[a,b], P. Govoni[a,b], L. Guzzi[a], M.T. Lucchini[a,b], M. Malberti[a], S. Malvezzi[a], A. Massironi[a], D. Menasce[a], L. Moroni[a], M. Paganoni[a,b], D. Pedrini[a], B.S. Pinolini[a], S. Ragazzi[a,b], N. Redaelli[a], T. Tabarelli de Fatis[a,b], D. Zuolo[a]

2024 JINST 19 P02031

INFN Sezione di Napoli[a], Università di Napoli 'Federico II'[b], Napoli, Italy; Università della Basilicata[c], Potenza, Italy; Università G. Marconi[d], Roma, Italy

S. Buontempo[a], A. Cagnotta[a,b], F. Carnevali[a,b], N. Cavallo[a,c], A. De Iorio[a,b], F. Fabozzi[a,c], A.O.M. Iorio[a,b], L. Lista[a,b,56], P. Paolucci[a,33], B. Rossi[a], C. Sciacca[a,b]

INFN Sezione di Padova[a], Università di Padova[b], Padova, Italy; Università di Trento[c], Trento, Italy

R. Ardino[a], P. Azzi[a], N. Bacchetta[a,57], D. Bisello[a,b], P. Bortignon[a], A. Bragagnolo[a,b], R. Carlin[a,b], P. Checchia[a], T. Dorigo[a], F. Gasparini[a,b], U. Gasparini[a,b], G. Grosso[a], L. Layer[a,58], E. Lusiani[a], M. Margoni[a,b], A.T. Meneguzzo[a,b], M. Migliorini[a,b], M. Passaseo[a], J. Pazzini[a,b], P. Ronchese[a,b], R. Rossin[a,b], F. Simonetto[a,b], G. Strong[a], M. Tosi[a,b], A. Triossi[a,b], S. Ventura[a], H. Yarar[a,b], M. Zanetti[a,b], P. Zotto[a,b], A. Zucchetta[a,b]

INFN Sezione di Pavia[a], Università di Pavia[b], Pavia, Italy

S. Abu Zeid[a,59], C. Aimè[a,b], A. Braghieri[a], S. Calzaferri[a,b], D. Fiorina[a,b], P. Montagna[a,b], V. Re[a], C. Riccardi[a,b], P. Salvini[a], I. Vai[a,b], P. Vitulo[a,b]

INFN Sezione di Perugia[a], Università di Perugia[b], Perugia, Italy

S. Ajmal[a,b], P. Asenov[a,60], G.M. Bilei[a], D. Ciangottini[a,b], L. Fanò[a,b], M. Magherini[a,b], G. Mantovani[a,b], V. Mariani[a,b], M. Menichelli[a], F. Moscatelli[a,60], A. Piccinelli[a,b], M. Presilla[a,b], A. Rossi[a,b], A. Santocchia[a,b], D. Spiga[a], T. Tedeschi[a,b]

INFN Sezione di Pisa[a], Università di Pisa[b], Scuola Normale Superiore di Pisa[c], Pisa, Italy; Università di Siena[d], Siena, Italy

P. Azzurri[a], G. Bagliesi[a], R. Bhattacharya[a], L. Bianchini[a,b], T. Boccali[a], E. Bossini[a], D. Bruschini[a,c], R. Castaldi[a], M.A. Ciocci[a,b], M. Cipriani[a,b], V. D'Amante[a,d], R. Dell'Orso[a], S. Donato[a], A. Giassi[a], F. Ligabue[a,c], D. Matos Figueiredo[a], A. Messineo[a,b], M. Musich[a,b], F. Palla[a], S. Parolia[a], A. Rizzi[a,b], G. Rolandi[a,c], S. Roy Chowdhury[a], T. Sarkar[a], A. Scribano[a], P. Spagnolo[a], R. Tenchini[a,b], G. Tonelli[a,b], N. Turini[a,d], A. Venturi[a], P.G. Verdini[a]

INFN Sezione di Roma[a], Sapienza Università di Roma[b], Roma, Italy

P. Barria[a], M. Campana[a,b], F. Cavallari[a], L. Cunqueiro Mendez[a,b], D. Del Re[a,b], E. Di Marco[a], M. Diemoz[a], F. Errico[a,b], E. Longo[a,b], P. Meridiani[a], J. Mijuskovic[a,b], G. Organtini[a,b], F. Pandolfi[a], R. Paramatti[a,b], C. Quaranta[a,b], S. Rahatlou[a,b], C. Rovelli[a], F. Santanastasio[a,b], L. Soffi[a], R. Tramontano[a,b]

INFN Sezione di Torino[a], Università di Torino[b], Torino, Italy; Università del Piemonte Orientale[c], Novara, Italy

N. Amapane[a,b], R. Arcidiacono[a,c], S. Argiro[a,b], M. Arneodo[a,c], N. Bartosik[a], R. Bellan[a,b], A. Bellora[a,b], C. Biino[a], N. Cartiglia[a], M. Costa[a,b], R. Covarelli[a,b], N. Demaria[a], L. Finco[a], M. Grippo[a,b], B. Kiani[a,b], F. Legger[a], F. Luongo[a,b], C. Mariotti[a], S. Maselli[a], A. Mecca[a,b], E. Migliore[a,b], M. Monteno[a], R. Mulargia[a], M.M. Obertino[a,b], G. Ortona[a], L. Pacher[a,b], N. Pastrone[a], M. Pelliccioni[a], M. Ruspa[a,c], F. Siviero[a,b], V. Sola[a,b],

2024 JINST 19 P02031

A. Solano[a,b], D. Soldi[a,b], A. Staiano[a], C. Tarricone[a,b], M. Tornago[a,b], D. Trocino[a], G. Umoret[a,b], E. Vlasov[a,b]

INFN Sezione di Trieste[a], Università di Trieste[b], Trieste, Italy

S. Belforte[a], V. Candelise[a,b], M. Casarsa[a], F. Cossutti[a], K. De Leo[a,b], G. Della Ricca[a,b]

Kyungpook National University, Daegu, Korea

S. Dogra, J. Hong, C. Huh, B. Kim, D.H. Kim, J. Kim, H. Lee, S.W. Lee, C.S. Moon, Y.D. Oh, M.S. Ryu, S. Sekmen, Y.C. Yang

Chonnam National University, Institute for Universe and Elementary Particles, Kwangju, Korea

G. Bak, P. Gwak, H. Kim, D.H. Moon

Hanyang University, Seoul, Korea

E. Asilar, D. Kim, T.J. Kim, J.A. Merlin, J. Park

Korea University, Seoul, Korea

S. Choi, S. Han, B. Hong, K. Lee, K.S. Lee, S. Lee, J. Park, S.K. Park, J. Yoo

Kyung Hee University, Department of Physics, Seoul, Korea

J. Goh

Sejong University, Seoul, Korea

H. S. Kim, Y. Kim, S. Lee

Seoul National University, Seoul, Korea

J. Almond, J.H. Bhyun, J. Choi, W. Jun, J. Kim, J.S. Kim, S. Ko, H. Kwon, H. Lee, J. Lee, J. Lee, B.H. Oh, S.B. Oh, H. Seo, U.K. Yang, I. Yoon

University of Seoul, Seoul, Korea

W. Jang, D.Y. Kang, Y. Kang, S. Kim, B. Ko, J.S.H. Lee, Y. Lee, I.C. Park, Y. Roh, I.J. Watson, S. Yang

Yonsei University, Department of Physics, Seoul, Korea

S. Ha, H.D. Yoo

Sungkyunkwan University, Suwon, Korea

M. Choi, M.R. Kim, H. Lee, Y. Lee, I. Yu

College of Engineering and Technology, American University of the Middle East (AUM), Dasman, Kuwait

T. Beyrouthy, Y. Maghrbi

Riga Technical University, Riga, Latvia

K. Dreimanis, A. Gaile, G. Pikurs, A. Potrebko, M. Seidel, V. Veckalns[61]

2024 JINST 19 P02031

University of Latvia (LU), Riga, Latvia
N.R. Strautnieks

Vilnius University, Vilnius, Lithuania
M. Ambrozas, A. Juodagalvis, A. Rinkevicius, G. Tamulaitis

National Centre for Particle Physics, Universiti Malaya, Kuala Lumpur, Malaysia
N. Bin Norjoharuddeen, I. Yusuff[62], Z. Zolkapli

Universidad de Sonora (UNISON), Hermosillo, Mexico
J.F. Benitez, A. Castaneda Hernandez, H.A. Encinas Acosta, L.G. Gallegos Maríñez, M. León Coello, J.A. Murillo Quijada, A. Sehrawat, L. Valencia Palomo

Centro de Investigacion y de Estudios Avanzados del IPN, Mexico City, Mexico
G. Ayala, H. Castilla-Valdez, E. De La Cruz-Burelo, I. Heredia-De La Cruz[63], R. Lopez-Fernandez, C.A. Mondragon Herrera, A. Sánchez Hernández

Universidad Iberoamericana, Mexico City, Mexico
C. Oropeza Barrera, M. Ramírez García

Benemerita Universidad Autonoma de Puebla, Puebla, Mexico
I. Bautista, I. Pedraza, H.A. Salazar Ibarguen, C. Uribe Estrada

University of Montenegro, Podgorica, Montenegro
I. Bubanja, N. Raicevic

University of Canterbury, Christchurch, New Zealand
P.H. Butler

National Centre for Physics, Quaid-I-Azam University, Islamabad, Pakistan
A. Ahmad, M.I. Asghar, A. Awais, M.I.M. Awan, H.R. Hoorani, W.A. Khan

AGH University of Krakow, Faculty of Computer Science, Electronics and Telecommunications, Krakow, Poland
V. Avati, L. Grzanka, M. Malawski

National Centre for Nuclear Research, Swierk, Poland
H. Bialkowska, M. Bluj, B. Boimska, M. Górski, M. Kazana, M. Szleper, P. Zalewski

Institute of Experimental Physics, Faculty of Physics, University of Warsaw, Warsaw, Poland
K. Bunkowski, K. Doroba, A. Kalinowski, M. Konecki, J. Krolikowski, A. Muhammad

Warsaw University of Technology, Warsaw, Poland
K. Pozniak, W. Zabolotny

2024 JINST 19 P02031

Laboratório de Instrumentação e Física Experimental de Partículas, Lisboa, Portugal
M. Araujo, D. Bastos, C. Beirão Da Cruz E Silva, A. Boletti, M. Bozzo, P. Faccioli, M. Gallinaro, J. Hollar, N. Leonardo, T. Niknejad, A. Petrilli, M. Pisano, J. Seixas, J. Varela, J.W. Wulff

Faculty of Physics, University of Belgrade, Belgrade, Serbia
P. Adzic, P. Milenovic

VINCA Institute of Nuclear Sciences, University of Belgrade, Belgrade, Serbia
M. Dordevic, J. Milosevic, V. Rekovic

Centro de Investigaciones Energéticas Medioambientales y Tecnológicas (CIEMAT), Madrid, Spain
M. Aguilar-Benitez, J. Alcaraz Maestre, Cristina F. Bedoya, M. Cepeda, M. Cerrada, N. Colino, B. De La Cruz, A. Delgado Peris, D. Fernández Del Val, J.P. Fernández Ramos, J. Flix, M.C. Fouz, O. Gonzalez Lopez, S. Goy Lopez, J.M. Hernandez, M.I. Josa, J. León Holgado, D. Moran, C. M. Morcillo Perez, Á. Navarro Tobar, C. Perez Dengra, A. Pérez-Calero Yzquierdo, J. Puerta Pelayo, I. Redondo, D.D. Redondo Ferrero, L. Romero, S. Sánchez Navas, L. Urda Gómez, J. Vazquez Escobar, C. Willmott

Universidad Autónoma de Madrid, Madrid, Spain
J.F. de Trocóniz

Universidad de Oviedo, Instituto Universitario de Ciencias y Tecnologías Espaciales de Asturias (ICTEA), Oviedo, Spain
B. Alvarez Gonzalez, J. Cuevas, J. Fernandez Menendez, S. Folgueras, I. Gonzalez Caballero, J.R. González Fernández, E. Palencia Cortezon, C. Ramón Álvarez, V. Rodríguez Bouza, A. Soto Rodríguez, A. Trapote, C. Vico Villalba, P. Vischia

Instituto de Física de Cantabria (IFCA), CSIC-Universidad de Cantabria, Santander, Spain
S. Bhowmik, S. Blanco Fernández, J.A. Brochero Cifuentes, I.J. Cabrillo, A. Calderon, J. Duarte Campderros, M. Fernandez, C. Fernandez Madrazo, G. Gomez, C. Lasaosa García, C. Martinez Rivero, P. Martinez Ruiz del Arbol, F. Matorras, P. Matorras Cuevas, E. Navarrete Ramos, J. Piedra Gomez, L. Scodellaro, I. Vila, J.M. Vizan Garcia

University of Colombo, Colombo, Sri Lanka
M.K. Jayananda, B. Kailasapathy[64], D.U.J. Sonnadara, D.D.C. Wickramarathna

University of Ruhuna, Department of Physics, Matara, Sri Lanka
W.G.D. Dharmaratna, K. Liyanage, N. Perera, N. Wickramage

CERN, European Organization for Nuclear Research, Geneva, Switzerland
D. Abbaneo, C. Amendola, E. Auffray, G. Auzinger, J. Baechler, D. Barney, A. Bermúdez Martínez, M. Bianco, B. Bilin, A.A. Bin Anuar, A. Bocci, E. Brondolin, C. Caillol, T. Camporesi, G. Cerminara, N. Chernyavskaya, D. d'Enterria, A. Dabrowski,

2024 JINST 19 P02031

A. David, A. De Roeck, M.M. Defranchis, M. Deile, M. Dobson, F. Fallavollita[65], L. Forthomme, G. Franzoni, W. Funk, S. Giani, D. Gigi, K. Gill, F. Glege, L. Gouskos, M. Haranko, J. Hegeman, V. Innocente, T. James, P. Janot, J. Kieseler, S. Laurila, P. Lecoq, E. Leutgeb, C. Lourenço, B. Maier, L. Malgeri, M. Mannelli, A.C. Marini, F. Meijers, S. Mersi, E. Meschi, V. Milosevic, F. Moortgat, M. Mulders, S. Orfanelli, F. Pantaleo, M. Peruzzi, G. Petrucciani, A. Pfeiffer, M. Pierini, D. Piparo, H. Qu, D. Rabady, G. Reales Gutiérrez, M. Rovere, H. Sakulin, S. Scarfi, M. Selvaggi, A. Sharma, K. Shchelina, P. Silva, P. Sphicas[66], A.G. Stahl Leiton, A. Steen, S. Summers, D. Treille, P. Tropea, A. Tsirou, D. Walter, J. Wanczyk[67], K.A. Wozniak[68], P. Zehetner, P. Zejdl, W.D. Zeuner

Paul Scherrer Institut, Villigen, Switzerland

T. Bevilacqua[69], L. Caminada[69], A. Ebrahimi, W. Erdmann, R. Horisberger, Q. Ingram, H.C. Kaestli, D. Kotlinski, C. Lange, M. Missiroli[69], L. Noehte[69], T. Rohe

ETH Zurich — Institute for Particle Physics and Astrophysics (IPA), Zurich, Switzerland

T.K. Aarrestad, K. Androsov[67], M. Backhaus, A. Calandri, C. Cazzaniga, K. Datta, A. De Cosa, G. Dissertori, M. Dittmar, M. Donegà, F. Eble, M. Galli, K. Gedia, F. Glessgen, C. Grab, D. Hits, W. Lustermann, A.-M. Lyon, R.A. Manzoni, M. Marchegiani, L. Marchese, C. Martin Perez, A. Mascellani[67], F. Nessi-Tedaldi, F. Pauss, V. Perovic, S. Pigazzini, M.G. Ratti, M. Reichmann, C. Reissel, T. Reitenspiess, B. Ristic, F. Riti, D. Ruini, D.A. Sanz Becerra, R. Seidita, J. Steggemann[67], D. Valsecchi, R. Wallny

Universität Zürich, Zurich, Switzerland

C. Amsler[70], P. Bärtschi, C. Botta, D. Brzhechko, M.F. Canelli, K. Cormier, R. Del Burgo, J.K. Heikkilä, M. Huwiler, W. Jin, A. Jofrehei, B. Kilminster, S. Leontsinis, S.P. Liechti, A. Macchiolo, P. Meiring, V.M. Mikuni, U. Molinatti, I. Neutelings, A. Reimers, P. Robmann, S. Sanchez Cruz, K. Schweiger, M. Senger, Y. Takahashi

National Central University, Chung-Li, Taiwan

C. Adloff[71], C.M. Kuo, W. Lin, P.K. Rout, P.C. Tiwari[43], S.S. Yu

National Taiwan University (NTU), Taipei, Taiwan

L. Ceard, Y. Chao, K.F. Chen, P.s. Chen, Z.g. Chen, W.-S. Hou, T.h. Hsu, Y.w. Kao, R. Khurana, G. Kole, Y.y. Li, R.-S. Lu, E. Paganis, A. Psallidas, X.f. Su, J. Thomas-Wilsker, H.y. Wu, E. Yazgan

High Energy Physics Research Unit, Department of Physics, Faculty of Science, Chulalongkorn University, Bangkok, Thailand

C. Asawatangtrakuldee, N. Srimanobhas, V. Wachirapusitanand

Çukurova University, Physics Department, Science and Art Faculty, Adana, Turkey

D. Agyel, F. Boran, Z.S. Demiroglu, F. Dolek, I. Dumanoglu[72], E. Eskut, Y. Guler[73], E. Gurpinar Guler[73], C. Isik, O. Kara, A. Kayis Topaksu, U. Kiminsu, G. Onengut, K. Ozdemir[74], A. Polatoz, B. Tali[75], U.G. Tok, S. Turkcapar, E. Uslan, I.S. Zorbakir

2024 JINST 19 P02031

Middle East Technical University, Physics Department, Ankara, Turkey
M. Yalvac[76]

Bogazici University, Istanbul, Turkey
B. Akgun, I.O. Atakisi, E. Gülmez, M. Kaya[77], O. Kaya[78], S. Tekten[79]

Istanbul Technical University, Istanbul, Turkey
A. Cakir, K. Cankocak[72], Y. Komurcu, S. Sen[80]

Istanbul University, Istanbul, Turkey
O. Aydilek, S. Cerci[75], V. Epshteyn, B. Hacisahinoglu, I. Hos[81], B. Isildak[82], B. Kaynak, S. Ozkorucuklu, O. Potok, H. Sert, C. Simsek, D. Sunar Cerci[75], C. Zorbilmez

Institute for Scintillation Materials of National Academy of Science of Ukraine, Kharkiv, Ukraine
A. Boyaryntsev, B. Grynyov

National Science Centre, Kharkiv Institute of Physics and Technology, Kharkiv, Ukraine
L. Levchuk

University of Bristol, Bristol, United Kingdom
D. Anthony, J.J. Brooke, A. Bundock, F. Bury, E. Clement, D. Cussans, H. Flacher, M. Glowacki, J. Goldstein, H.F. Heath, L. Kreczko, B. Krikler, S. Paramesvaran, S. Seif El Nasr-Storey, V.J. Smith, N. Stylianou[83], K. Walkingshaw Pass, R. White

Rutherford Appleton Laboratory, Didcot, United Kingdom
A.H. Ball, K.W. Bell, A. Belyaev[84], C. Brew, R.M. Brown, D.J.A. Cockerill, C. Cooke, K.V. Ellis, K. Harder, S. Harper, M.-L. Holmberg[85], J. Linacre, K. Manolopoulos, D.M. Newbold, E. Olaiya, D. Petyt, T. Reis, G. Salvi, T. Schuh, C.H. Shepherd-Themistocleous, I.R. Tomalin, T. Williams

Imperial College, London, United Kingdom
R. Bainbridge, P. Bloch, C.E. Brown, O. Buchmuller, V. Cacchio, C.A. Carrillo Montoya, G.S. Chahal[86], D. Colling, J.S. Dancu, P. Dauncey, G. Davies, J. Davies, M. Della Negra, S. Fayer, G. Fedi, G. Hall, M.H. Hassanshahi, A. Howard, G. Iles, M. Knight, J. Langford, L. Lyons, A.-M. Magnan, S. Malik, A. Martelli, M. Mieskolainen, J. Nash[87], M. Pesaresi, B.C. Radburn-Smith, A. Richards, A. Rose, C. Seez, R. Shukla, A. Tapper, K. Uchida, G.P. Uttley, L.H. Vage, T. Virdee[33], M. Vojinovic, N. Wardle, D. Winterbottom

Brunel University, Uxbridge, United Kingdom
K. Coldham, J.E. Cole, A. Khan, P. Kyberd, I.D. Reid

Baylor University, Waco, Texas, U.S.A.
S. Abdullin, A. Brinkerhoff, B. Caraway, J. Dittmann, K. Hatakeyama, J. Hiltbrand, A.R. Kanuganti, B. McMaster, M. Saunders, S. Sawant, C. Sutantawibul, M. Toms[88], J. Wilson

2024 JINST 19 P02031

Catholic University of America, Washington, DC, U.S.A.
R. Bartek, A. Dominguez, C. Huerta Escamilla, A.E. Simsek, R. Uniyal, A.M. Vargas Hernandez

The University of Alabama, Tuscaloosa, Alabama, U.S.A.
R. Chudasama, S.I. Cooper, S.V. Gleyzer, C.U. Perez, P. Rumerio[89], E. Usai, C. West, R. Yi

Boston University, Boston, Massachusetts, U.S.A.
A. Akpinar, A. Albert, D. Arcaro, C. Cosby, Z. Demiragli, C. Erice, E. Fontanesi, D. Gastler, S. Jeon, J. Rohlf, K. Salyer, D. Sperka, D. Spitzbart, I. Suarez, A. Tsatsos, S. Yuan

Brown University, Providence, Rhode Island, U.S.A.
G. Benelli, X. Coubez[28], D. Cutts, M. Hadley, U. Heintz, J.M. Hogan[90], T. Kwon, G. Landsberg, K.T. Lau, D. Li, J. Luo, S. Mondal, M. Narain[†], N. Pervan, S. Sagir[91], F. Simpson, M. Stamenkovic, W.Y. Wong, X. Yan, W. Zhang

University of California, Davis, Davis, California, U.S.A.
S. Abbott, J. Bonilla, C. Brainerd, R. Breedon, M. Calderon De La Barca Sanchez, M. Chertok, M. Citron, J. Conway, P.T. Cox, R. Erbacher, F. Jensen, O. Kukral, G. Mocellin, M. Mulhearn, D. Pellett, W. Wei, Y. Yao, F. Zhang

University of California, Los Angeles, California, U.S.A.
M. Bachtis, R. Cousins, A. Datta, J. Hauser, M. Ignatenko, M.A. Iqbal, T. Lam, E. Manca, W.A. Nash, D. Saltzberg, B. Stone, V. Valuev

University of California, Riverside, Riverside, California, U.S.A.
R. Clare, M. Gordon, G. Hanson, W. Si, S. Wimpenny[†]

University of California, San Diego, La Jolla, California, U.S.A.
J.G. Branson, S. Cittolin, S. Cooperstein, D. Diaz, J. Duarte, R. Gerosa, L. Giannini, J. Guiang, R. Kansal, V. Krutelyov, R. Lee, J. Letts, M. Masciovecchio, F. Mokhtar, M. Pieri, M. Quinnan, B.V. Sathia Narayanan, V. Sharma, M. Tadel, E. Vourliotis, F. Würthwein, Y. Xiang, A. Yagil

University of California, Santa Barbara — Department of Physics, Santa Barbara, California, U.S.A.
A. Barzdukas, L. Brennan, C. Campagnari, G. Collura, A. Dorsett, J. Incandela, M. Kilpatrick, J. Kim, A.J. Li, P. Masterson, H. Mei, M. Oshiro, J. Richman, U. Sarica, R. Schmitz, F. Setti, J. Sheplock, D. Stuart, S. Wang

California Institute of Technology, Pasadena, California, U.S.A.
A. Bornheim, O. Cerri, A. Latorre, J.M. Lawhorn, J. Mao, H.B. Newman, T. Q. Nguyen, M. Spiropulu, J.R. Vlimant, C. Wang, S. Xie, R.Y. Zhu

2024 JINST 19 P02031

Carnegie Mellon University, Pittsburgh, Pennsylvania, U.S.A.

J. Alison, S. An, M.B. Andrews, P. Bryant, V. Dutta, T. Ferguson, A. Harilal, C. Liu, T. Mudholkar, S. Murthy, M. Paulini, A. Roberts, A. Sanchez, W. Terrill

University of Colorado Boulder, Boulder, Colorado, U.S.A.

J.P. Cumalat, W.T. Ford, A. Hassani, G. Karathanasis, E. MacDonald, N. Manganelli, F. Marini, A. Perloff, C. Savard, N. Schonbeck, K. Stenson, K.A. Ulmer, S.R. Wagner, N. Zipper

Cornell University, Ithaca, New York, U.S.A.

J. Alexander, S. Bright-Thonney, X. Chen, D.J. Cranshaw, J. Fan, X. Fan, D. Gadkari, S. Hogan, J. Monroy, J.R. Patterson, J. Reichert, M. Reid, A. Ryd, J. Thom, P. Wittich, R. Zou

Fermi National Accelerator Laboratory, Batavia, Illinois, U.S.A.

M. Albrow, M. Alyari, O. Amram, G. Apollinari, A. Apresyan, L.A.T. Bauerdick, D. Berry, J. Berryhill, P.C. Bhat, K. Burkett, J.N. Butler, A. Canepa, G.B. Cerati, H.W.K. Cheung, F. Chlebana, G. Cummings, J. Dickinson, I. Dutta, V.D. Elvira, Y. Feng, J. Freeman, A. Gandrakota, Z. Gecse, L. Gray, D. Green, A. Grummer, S. Grünendahl, D. Guerrero, O. Gutsche, R.M. Harris, R. Heller, T.C. Herwig, J. Hirschauer, L. Horyn, B. Jayatilaka, S. Jindariani, M. Johnson, U. Joshi, T. Klijnsma, B. Klima, K.H.M. Kwok, S. Lammel, D. Lincoln, R. Lipton, T. Liu, C. Madrid, K. Maeshima, C. Mantilla, D. Mason, P. McBride, P. Merkel, S. Mrenna, S. Nahn, J. Ngadiuba, D. Noonan, V. Papadimitriou, N. Pastika, K. Pedro, C. Pena[92], F. Ravera, A. Reinsvold Hall[93], L. Ristori, E. Sexton-Kennedy, N. Smith, A. Soha, L. Spiegel, S. Stoynev, J. Strait, L. Taylor, S. Tkaczyk, N.V. Tran, L. Uplegger, E.W. Vaandering, I. Zoi

University of Florida, Gainesville, Florida, U.S.A.

C. Aruta, P. Avery, D. Bourilkov, L. Cadamuro, P. Chang, V. Cherepanov, R.D. Field, E. Koenig, M. Kolosova, J. Konigsberg, A. Korytov, K.H. Lo, K. Matchev, N. Menendez, G. Mitselmakher, A. Muthirakalayil Madhu, N. Rawal, D. Rosenzweig, S. Rosenzweig, K. Shi, J. Wang

Florida State University, Tallahassee, Florida, U.S.A.

T. Adams, A. Al Kadhim, A. Askew, N. Bower, R. Habibullah, V. Hagopian, R. Hashmi, R.S. Kim, S. Kim, T. Kolberg, G. Martinez, H. Prosper, P.R. Prova, O. Viazlo, M. Wulansatiti, R. Yohay, J. Zhang

Florida Institute of Technology, Melbourne, Florida, U.S.A.

B. Alsufyani, M.M. Baarmand, S. Butalla, T. Elkafrawy[59], M. Hohlmann, R. Kumar Verma, M. Rahmani

University of Illinois Chicago, Chicago, U.S.A., Chicago, U.S.A.

M.R. Adams, C. Bennett, R. Cavanaugh, S. Dittmer, R. Escobar Franco, O. Evdokimov, C.E. Gerber, D.J. Hofman, J.h. Lee, D. S. Lemos, A.H. Merrit, C. Mills, S. Nanda, G. Oh,

2024 JINST 19 P02031

B. Ozek, D. Pilipovic, T. Roy, S. Rudrabhatla, M.B. Tonjes, N. Varelas, X. Wang, Z. Ye, J. Yoo

The University of Iowa, Iowa City, Iowa, U.S.A.

M. Alhusseini, D. Blend, K. Dilsiz[94], L. Emediato, G. Karaman, O.K. Köseyan, J.-P. Merlo, A. Mestvirishvili[95], J. Nachtman, O. Neogi, H. Ogul[96], Y. Onel, A. Penzo, C. Snyder, E. Tiras[97]

Johns Hopkins University, Baltimore, Maryland, U.S.A.

B. Blumenfeld, L. Corcodilos, J. Davis, A.V. Gritsan, L. Kang, S. Kyriacou, P. Maksimovic, M. Roguljic, J. Roskes, S. Sekhar, M. Swartz, T.Á. Vámi

The University of Kansas, Lawrence, Kansas, U.S.A.

A. Abreu, L.F. Alcerro Alcerro, J. Anguiano, P. Baringer, A. Bean, Z. Flowers, D. Grove, J. King, G. Krintiras, M. Lazarovits, C. Le Mahieu, C. Lindsey, J. Marquez, N. Minafra, M. Murray, M. Nickel, M. Pitt, S. Popescu[98], C. Rogan, C. Royon, R. Salvatico, S. Sanders, C. Smith, Q. Wang, G. Wilson

Kansas State University, Manhattan, Kansas, U.S.A.

B. Allmond, A. Ivanov, K. Kaadze, A. Kalogeropoulos, D. Kim, Y. Maravin, K. Nam, J. Natoli, D. Roy, G. Sorrentino

Lawrence Livermore National Laboratory, Livermore, California, U.S.A.

F. Rebassoo, D. Wright

University of Maryland, College Park, Maryland, U.S.A.

E. Adams, A. Baden, O. Baron, A. Belloni, A. Bethani, Y.M. Chen, S.C. Eno, N.J. Hadley, S. Jabeen, R.G. Kellogg, T. Koeth, Y. Lai, S. Lascio, A.C. Mignerey, S. Nabili, C. Palmer, C. Papageorgakis, M.M. Paranjpe, L. Wang, K. Wong

Massachusetts Institute of Technology, Cambridge, Massachusetts, U.S.A.

J. Bendavid, W. Busza, I.A. Cali, Y. Chen, M. D'Alfonso, J. Eysermans, C. Freer, G. Gomez-Ceballos, M. Goncharov, P. Harris, D. Hoang, D. Kovalskyi, J. Krupa, L. Lavezzo, Y.-J. Lee, K. Long, C. Mironov, C. Paus, D. Rankin, C. Roland, G. Roland, S. Rothman, Z. Shi, G.S.F. Stephans, J. Wang, Z. Wang, B. Wyslouch, T. J. Yang

University of Minnesota, Minneapolis, Minnesota, U.S.A.

B. Crossman, B.M. Joshi, C. Kapsiak, M. Krohn, D. Mahon, J. Mans, B. Marzocchi, S. Pandey, M. Revering, R. Rusack, R. Saradhy, N. Schroeder, N. Strobbe, M.A. Wadud

University of Mississippi, Oxford, Mississippi, U.S.A.

L.M. Cremaldi

University of Nebraska-Lincoln, Lincoln, Nebraska, U.S.A.

K. Bloom, M. Bryson, D.R. Claes, C. Fangmeier, F. Golf, G. Haza, J. Hossain, C. Joo, I. Kravchenko, I. Reed, J.E. Siado, W. Tabb, A. Vagnerini, A. Wightman, F. Yan, D. Yu, A.G. Zecchinelli

2024 JINST 19 P02031

State University of New York at Buffalo, Buffalo, New York, U.S.A.
G. Agarwal, H. Bandyopadhyay, L. Hay, I. Iashvili, A. Kharchilava, C. McLean, M. Morris, D. Nguyen, S. Rappoccio, H. Rejeb Sfar, A. Williams

Northeastern University, Boston, Massachusetts, U.S.A.
G. Alverson, E. Barberis, Y. Haddad, Y. Han, A. Krishna, J. Li, M. Lu, G. Madigan, D.M. Morse, V. Nguyen, T. Orimoto, A. Parker, L. Skinnari, A. Tishelman-Charny, B. Wang, D. Wood

Northwestern University, Evanston, Illinois, U.S.A.
S. Bhattacharya, J. Bueghly, Z. Chen, K.A. Hahn, Y. Liu, Y. Miao, D.G. Monk, M.H. Schmitt, A. Taliercio, M. Velasco

University of Notre Dame, Notre Dame, Indiana, U.S.A.
R. Band, R. Bucci, S. Castells, M. Cremonesi, A. Das, R. Goldouzian, M. Hildreth, K.W. Ho, K. Hurtado Anampa, C. Jessop, K. Lannon, J. Lawrence, N. Loukas, L. Lutton, J. Mariano, N. Marinelli, I. Mcalister, T. McCauley, C. Mcgrady, K. Mohrman, C. Moore, Y. Musienko[16], H. Nelson, M. Osherson, R. Ruchti, A. Townsend, M. Wayne, H. Yockey, M. Zarucki, L. Zygala

The Ohio State University, Columbus, Ohio, U.S.A.
A. Basnet, B. Bylsma, M. Carrigan, L.S. Durkin, C. Hill, M. Joyce, A. Lesauvage, M. Nunez Ornelas, K. Wei, B.L. Winer, B. R. Yates

Princeton University, Princeton, New Jersey, U.S.A.
F.M. Addesa, H. Bouchamaoui, P. Das, G. Dezoort, P. Elmer, A. Frankenthal, B. Greenberg, N. Haubrich, S. Higginbotham, G. Kopp, S. Kwan, D. Lange, A. Loeliger, D. Marlow, I. Ojalvo, J. Olsen, D. Stickland, C. Tully

University of Puerto Rico, Mayaguez, Puerto Rico, U.S.A.
S. Malik

Purdue University, West Lafayette, Indiana, U.S.A.
A.S. Bakshi, V.E. Barnes, S. Chandra, R. Chawla, S. Das, A. Gu, L. Gutay, M. Jones, A.W. Jung, D. Kondratyev, A.M. Koshy, M. Liu, G. Negro, N. Neumeister, G. Paspalaki, S. Piperov, V. Scheurer, J.F. Schulte, M. Stojanovic, J. Thieman, A. K. Virdi, F. Wang, W. Xie

Purdue University Northwest, Hammond, Indiana, U.S.A.
J. Dolen, N. Parashar, A. Pathak

Rice University, Houston, Texas, U.S.A.
D. Acosta, A. Baty, T. Carnahan, S. Dildick, K.M. Ecklund, P.J. Fernández Manteca, S. Freed, P. Gardner, F.J.M. Geurts, A. Kumar, W. Li, O. Miguel Colin, B.P. Padley, R. Redjimi, J. Rotter, E. Yigitbasi, Y. Zhang

2024 JINST 19 P02031

University of Rochester, Rochester, New York, U.S.A.

A. Bodek, P. de Barbaro, R. Demina, J.L. Dulemba, C. Fallon, A. Garcia-Bellido, O. Hindrichs, A. Khukhunaishvili, P. Parygin[88], E. Popova[88], R. Taus, G.P. Van Onsem

The Rockefeller University, New York, New York, U.S.A.

K. Goulianos

Rutgers, The State University of New Jersey, Piscataway, New Jersey, U.S.A.

B. Chiarito, J.P. Chou, Y. Gershtein, E. Halkiadakis, A. Hart, M. Heindl, D. Jaroslawski, O. Karacheban[31], I. Laflotte, A. Lath, R. Montalvo, K. Nash, H. Routray, S. Salur, S. Schnetzer, S. Somalwar, R. Stone, S.A. Thayil, S. Thomas, J. Vora, H. Wang

University of Tennessee, Knoxville, Tennessee, U.S.A.

H. Acharya, D. Ally, A.G. Delannoy, S. Fiorendi, T. Holmes, N. Karunarathna, L. Lee, E. Nibigira, S. Spanier

Texas A&M University, College Station, Texas, U.S.A.

D. Aebi, M. Ahmad, O. Bouhali[99], M. Dalchenko, R. Eusebi, J. Gilmore, T. Huang, T. Kamon[100], H. Kim, S. Luo, S. Malhotra, R. Mueller, D. Overton, D. Rathjens, A. Safonov

Texas Tech University, Lubbock, Texas, U.S.A.

N. Akchurin, J. Damgov, V. Hegde, A. Hussain, Y. Kazhykarim, K. Lamichhane, S.W. Lee, A. Mankel, T. Mengke, S. Muthumuni, T. Peltola, I. Volobouev, A. Whitbeck

Vanderbilt University, Nashville, Tennessee, U.S.A.

E. Appelt, S. Greene, A. Gurrola, W. Johns, R. Kunnawalkam Elayavalli, A. Melo, F. Romeo, P. Sheldon, S. Tuo, J. Velkovska, J. Viinikainen

University of Virginia, Charlottesville, Virginia, U.S.A.

B. Cardwell, B. Cox, J. Hakala, R. Hirosky, A. Ledovskoy, A. Li, C. Neu, C.E. Perez Lara

Wayne State University, Detroit, Michigan, U.S.A.

P.E. Karchin

University of Wisconsin — Madison, Madison, Wisconsin, U.S.A.

A. Aravind, S. Banerjee, K. Black, T. Bose, S. Dasu, I. De Bruyn, P. Everaerts, C. Galloni, H. He, M. Herndon, A. Herve, C.K. Koraka, A. Lanaro, R. Loveless, J. Madhusudanan Sreekala, A. Mallampalli, A. Mohammadi, S. Mondal, G. Parida, D. Pinna, A. Savin, V. Shang, V. Sharma, W.H. Smith, D. Teague, H.F. Tsoi, W. Vetens, A. Warden

Authors affiliated with an institute or an international laboratory covered by a cooperation agreement with CERN

S. Afanasiev, V. Andreev, Yu. Andreev, T. Aushev, M. Azarkin, A. Babaev, A. Belyaev, V. Blinov[101], E. Boos, V. Borshch, D. Budkouski, M. Chadeeva[101], V. Chekhovsky, M. Danilov[101], A. Demiyanov, A. Dermenev, T. Dimova[101], D. Druzhkin[102], M. Dubinin[92], L. Dudko, A. Ershov, G. Gavrilov, V. Gavrilov, S. Gninenko, V. Golovtcov, N. Golubev,

2024 JINST 19 P02031

I. Golutvin, I. Gorbunov, A. Gribushin, Y. Ivanov, V. Kachanov, L. Kardapoltsev[101], V. Karjavine, A. Karneyeu, V. Kim[101], M. Kirakosyan, D. Kirpichnikov, M. Kirsanov, V. Klyukhin, O. Kodolova[103], D. Konstantinov, V. Korenkov, A. Kozyrev[101], N. Krasnikov, A. Lanev, P. Levchenko[104], N. Lychkovskaya, V. Makarenko, A. Malakhov, V. Matveev[101], V. Murzin, A. Nikitenko[105,103], S. Obraztsov, V. Oreshkin, V. Palichik, V. Perelygin, S. Petrushanko, S. Polikarpov[101], V. Popov, O. Radchenko[101], M. Savina, V. Savrin, V. Shalaev, S. Shmatov, S. Shulha, Y. Skovpen[101], S. Slabospitskii, V. Smirnov, A. Snigirev, D. Sosnov, V. Sulimov, E. Tcherniaev, A. Terkulov, O. Teryaev, I. Tlisova, A. Toropin, L. Uvarov, A. Uzunian, A. Vorobyev[†], N. Voytishin, B.S. Yuldashev[106], A. Zarubin, I. Zhizhin, A. Zhokin

[†] *Deceased.*
[1] *Also at Yerevan State University, Yerevan, Armenia*
[2] *Also at TU Wien, Vienna, Austria*
[3] *Also at Institute of Basic and Applied Sciences, Faculty of Engineering, Arab Academy for Science, Technology and Maritime Transport, Alexandria, Egypt*
[4] *Also at Ghent University, Ghent, Belgium*
[5] *Also at Universidade Estadual de Campinas, Campinas, Brazil*
[6] *Also at Federal University of Rio Grande do Sul, Porto Alegre, Brazil*
[7] *Also at UFMS, Nova Andradina, Brazil*
[8] *Also at Nanjing Normal University, Nanjing, China*
[9] *Now at Henan Normal University, Xinxiang, China*
[10] *Now at The University of Iowa, Iowa City, Iowa, U.S.A.*
[11] *Also at University of Chinese Academy of Sciences, Beijing, China*
[12] *Also at China Center of Advanced Science and Technology, Beijing, China*
[13] *Also at University of Chinese Academy of Sciences, Beijing, China*
[14] *Also at China Spallation Neutron Source, Guangdong, China*
[15] *Also at Université Libre de Bruxelles, Bruxelles, Belgium*
[16] *Also at an institute or an international laboratory covered by a cooperation agreement with CERN*
[17] *Also at Cairo University, Cairo, Egypt*
[18] *Also at Suez University, Suez, Egypt*
[19] *Now at British University in Egypt, Cairo, Egypt*
[20] *Also at Birla Institute of Technology, Mesra, Mesra, India*
[21] *Also at Purdue University, West Lafayette, Indiana, U.S.A.*
[22] *Also at Université de Haute Alsace, Mulhouse, France*
[23] *Also at Department of Physics, Tsinghua University, Beijing, China*
[24] *Also at Ilia State University, Tbilisi, Georgia*
[25] *Also at The University of the State of Amazonas, Manaus, Brazil*
[26] *Also at Erzincan Binali Yildirim University, Erzincan, Turkey*
[27] *Also at University of Hamburg, Hamburg, Germany*
[28] *Also at RWTH Aachen University, III. Physikalisches Institut A, Aachen, Germany*
[29] *Also at Isfahan University of Technology, Isfahan, Iran*
[30] *Also at Bergische University Wuppertal (BUW), Wuppertal, Germany*
[31] *Also at Brandenburg University of Technology, Cottbus, Germany*
[32] *Also at Forschungszentrum Jülich, Juelich, Germany*
[33] *Also at CERN, European Organization for Nuclear Research, Geneva, Switzerland*
[34] *Also at Institute of Physics, University of Debrecen, Debrecen, Hungary*
[35] *Also at Institute of Nuclear Research ATOMKI, Debrecen, Hungary*
[36] *Now at Universitatea Babes-Bolyai — Facultatea de Fizica, Cluj-Napoca, Romania*
[37] *Also at Physics Department, Faculty of Science, Assiut University, Assiut, Egypt*
[38] *Also at HUN-REN Wigner Research Centre for Physics, Budapest, Hungary*
[39] *Also at Faculty of Informatics, University of Debrecen, Debrecen, Hungary*

2024 JINST 19 P02031

[40] *Also at Punjab Agricultural University, Ludhiana, India*
[41] *Also at University of Hyderabad, Hyderabad, India*
[42] *Also at University of Visva-Bharati, Santiniketan, India*
[43] *Also at Indian Institute of Science (IISc), Bangalore, India*
[44] *Also at IIT Bhubaneswar, Bhubaneswar, India*
[45] *Also at Institute of Physics, Bhubaneswar, India*
[46] *Also at Deutsches Elektronen-Synchrotron, Hamburg, Germany*
[47] *Also at Department of Physics, Isfahan University of Technology, Isfahan, Iran*
[48] *Also at Sharif University of Technology, Tehran, Iran*
[49] *Also at Department of Physics, University of Science and Technology of Mazandaran, Behshahr, Iran*
[50] *Also at Helwan University, Cairo, Egypt*
[51] *Also at Italian National Agency for New Technologies, Energy and Sustainable Economic Development, Bologna, Italy*
[52] *Also at Centro Siciliano di Fisica Nucleare e di Struttura Della Materia, Catania, Italy*
[53] *Also at ENEA — Casaccia Research Center, S. Maria di Galeria, Italy*
[54] *Also at Università degli Studi Guglielmo Marconi, Roma, Italy*
[55] *Also at Facoltà Ingegneria, Università di Roma, Roma, Italy*
[56] *Also at Scuola Superiore Meridionale, Università di Napoli 'Federico II', Napoli, Italy*
[57] *Also at Fermi National Accelerator Laboratory, Batavia, Illinois, U.S.A.*
[58] *Also at Università di Napoli 'Federico II', Napoli, Italy*
[59] *Also at Ain Shams University, Cairo, Egypt*
[60] *Also at Consiglio Nazionale delle Ricerche — Istituto Officina dei Materiali, Perugia, Italy*
[61] *Also at Riga Technical University, Riga, Latvia*
[62] *Also at Department of Applied Physics, Faculty of Science and Technology, Universiti Kebangsaan Malaysia, Bangi, Malaysia*
[63] *Also at Consejo Nacional de Ciencia y Tecnología, Mexico City, Mexico*
[64] *Also at Trincomalee Campus, Eastern University, Sri Lanka, Nilaveli, Sri Lanka*
[65] *Also at INFN Sezione di Pavia, Università di Pavia, Pavia, Italy*
[66] *Also at National and Kapodistrian University of Athens, Athens, Greece*
[67] *Also at Ecole Polytechnique Fédérale Lausanne, Lausanne, Switzerland*
[68] *Also at University of Vienna Faculty of Computer Science, Vienna, Austria*
[69] *Also at Universität Zürich, Zurich, Switzerland*
[70] *Also at Stefan Meyer Institute for Subatomic Physics, Vienna, Austria*
[71] *Also at Laboratoire d'Annecy-le-Vieux de Physique des Particules, IN2P3-CNRS, Annecy-le-Vieux, France*
[72] *Also at Near East University, Research Center of Experimental Health Science, Mersin, Turkey*
[73] *Also at Konya Technical University, Konya, Turkey*
[74] *Also at Izmir Bakircay University, Izmir, Turkey*
[75] *Also at Adiyaman University, Adiyaman, Turkey*
[76] *Also at Bozok Universitetesi Rektörlügü, Yozgat, Turkey*
[77] *Also at Marmara University, Istanbul, Turkey*
[78] *Also at Milli Savunma University, Istanbul, Turkey*
[79] *Also at Kafkas University, Kars, Turkey*
[80] *Also at Hacettepe University, Ankara, Turkey*
[81] *Also at Istanbul University — Cerrahpasa, Faculty of Engineering, Istanbul, Turkey*
[82] *Also at Yildiz Technical University, Istanbul, Turkey*
[83] *Also at Vrije Universiteit Brussel, Brussel, Belgium*
[84] *Also at School of Physics and Astronomy, University of Southampton, Southampton, United Kingdom*
[85] *Also at University of Bristol, Bristol, United Kingdom*
[86] *Also at IPPP Durham University, Durham, United Kingdom*
[87] *Also at Monash University, Faculty of Science, Clayton, Australia*
[88] *Now at an institute or an international laboratory covered by a cooperation agreement with CERN*
[89] *Also at Università di Torino, Torino, Italy*

2024 JINST 19 P02031

[90] *Also at Bethel University, St. Paul, Minnesota, U.S.A.*
[91] *Also at Karamanoğlu Mehmetbey University, Karaman, Turkey*
[92] *Also at California Institute of Technology, Pasadena, California, U.S.A.*
[93] *Also at United States Naval Academy, Annapolis, Maryland, U.S.A.*
[94] *Also at Bingol University, Bingol, Turkey*
[95] *Also at Georgian Technical University, Tbilisi, Georgia*
[96] *Also at Sinop University, Sinop, Turkey*
[97] *Also at Erciyes University, Kayseri, Turkey*
[98] *Also at Horia Hulubei National Institute of Physics and Nuclear Engineering (IFIN-HH), Bucharest, Romania*
[99] *Also at Texas A&M University at Qatar, Doha, Qatar*
[100] *Also at Kyungpook National University, Daegu, Korea*
[101] *Also at another institute or international laboratory covered by a cooperation agreement with CERN*
[102] *Also at Universiteit Antwerpen, Antwerpen, Belgium*
[103] *Also at Yerevan Physics Institute, Yerevan, Armenia*
[104] *Also at Northeastern University, Boston, Massachusetts, U.S.A.*
[105] *Also at Imperial College, London, United Kingdom*
[106] *Also at Institute of Nuclear Physics of the Uzbekistan Academy of Sciences, Tashkent, Uzbekistan*

2024 JINST 19 P02031